antagonists on inflammatory hyperalgesia in the rat. Br J Pharmacol 117:196–202.

Rexed B (1952) The cytoarchitectonic organization of the spinal cord in the cat. J Comp Neurol 96:414–495.

Sangameswaran L, Delgado SG, Fish LM, Koch BD, Jakeman LB, Stewart GR, Sze P, Hunter JC, Eglen RM, Herman RC (1996) Structure and function of a novel voltage-gated, tetrodotoxin-resistant sodium channel specific to sensory neurons. J Biol Chem 271:5953–5956.

Schaller KL, Krzemien DM, Yarowsky PJ, Krueger BK, Caldwell JH (1995) A novel, abundant sodium channel expressed in neurons and glia. J Neurosci 15:3231–3242.

Suzuki R, Dickenson AH (2006) Differential pharmacological modulation of the spontaneous stimulus-independent activity in the rat spinal cord following peripheral nerve injury. Exp Neurol 198: 72–80.

Toledo-Aral JJ, Moss BL, He ZJ, Koszowski AG, Whisenand T, Levinson SR, Wolf JJ, Silos-Santiago I, Halegoua S, Mandel G (1997) Identification of PN1, a predominant voltage-dependent sodium channel expressed principally in peripheral neurons. Proc Natl Acad Sci U S A 94:1527–1532.

Tyrrell L, Renganathan M, Dib-Hajj SD, Waxman SG (2001) Glycosylation alters steady-state inactivation of sodium channel Nav1.9/NaN in dorsal root ganglion neurons and is developmentally regulated. J Neurosci 21:9629–9637.

Tzoumaka E, Tischler AC, Sangameswaran L, Eglen RM, Hunter JC, Novakovic SD (2000) Differential distribution of the tetrodotoxin-sensitive rPN4/NaCh6/Scn8a sodium channel in the nervous system. J Neurosci Res 60:37–44.

Vijayaragavan K, Boutjdir M, Chahine M (2004) Modulation of Nav1.7 and Nav1.8 peripheral nerve sodium channels by protein kinase A and protein kinase C. J Neurophysiol 91:1556–1569.

Westenbroek RE, Merrick DK, Catterall WA (1989) Differential subcellular localization of the RI and RII Na+ channel subtypes in central neurons. Neuron 3:695–704.

Willis WD Jr, Coggeshall ER (2004) Sensrory mechanisms of the spinal cord; primary afferent neurons and the spinal dorsal horn. New York, NY: Kluwer Academic/Plenum Publishers.

Wittmack EK, Rush AM, Craner MJ, Goldfarb M, Waxman SG, Dib-Hajj SD (2004) Fibroblast growth factor homologous factor 2B: association with Nav1.6 and selective colocalization at nodes of Ranvier of dorsal root axons. J Neurosci 24:6765–6775.

Wittmack EK, Rush AM, Hudmon A, Waxman SG, Dib-Hajj SD (2005) Voltage-gated sodium channel Nav1.6 is modulated by p38 mitogen-activated protein kinase. J Neurosci 25:6621–6630.

Wu LJ, Duan B, Mei YD, Gao J, Chen JG, Zhuo M, Xu L, Wu M, Xu TL (2004) Characterization of acid-sensing ion channels in dorsal horn neurons of rat spinal cord. J Biol Chem 279:43716–43724.

(Accepted 25 May 2010)
(Available online 31 May 2010)

Okubo et al. Molecular Pain 2010, 6:57
http://www.molecularpain.com/content/6/1/57

MOLECULAR PAIN

RESEARCH Open Access

Expression of leukotriene receptors in the rat dorsal root ganglion and the effects on pain behaviors

Masamichi Okubo[1], Hiroki Yamanaka[1], Kimiko Kobayashi[1], Tetsuo Fukuoka[1], Yi Dai[2], Koichi Noguchi[1*]

Abstract

Background: Leukotrienes (LTs) belong to the large family of lipid mediators implicated in various inflammatory conditions such as asthma and rheumatoid arthritis. Four distinct types (BLT1, BLT2, CysLT1 and CysLT2) of G-protein-coupled receptors for LTs have been identified. Several studies have reported that LTs are involved in inflammatory pain, but the mechanism and the expression of LT receptors in the nociceptive pathway are unknown.

Results: We investigated the precise expression of these four types of LT receptors in the adult rat dorsal root ganglion (DRG) using reverse transcription-polymerase reaction (RT-PCR) and radioisotope-labeled *in situ* hybridization histochemistry (ISHH). We detected mRNAs for BLT1 and CysLT2 in the DRG, but not for BLT2 and CysLT1. CysLT2 mRNA was preferentially expressed by small sized DRG neurons (about 36% of total neurons), whereas BLT1 mRNA was expressed by non-neuronal cells. Double labeling analysis of CysLT2 with NF-200, calcitonin gene-related peptide (CGRP), isolectin B4 (IB4), transient receptor potential vanilloid subfamily 1 (TRPV1) and P2X3 receptor revealed that many CysLT2-labeled neurons were localized with unmyelinated and non-peptidergic neurons, and interestingly, CysLT2 mRNA heavily co-localized with TRPV1 and P2X3-positive neurons. Intraplantar injection of LTC4, a CysLT2 receptor agonist, itself did not induce the thermal hyperalgesia, spontaneous pain behaviors or swelling of hind paw. However, pretreatment of LTC4 remarkably enhanced the painful behaviors produced by alpha, beta-methylene adenosine 5'-triphosphate ($\alpha\beta$-me-ATP), a P2X3 receptor agonist.

Conclusions: These data suggests that CysLT2 expressed in DRG neurons may play a role as a modulator of P2X3, and contribute to a potentiation of the neuronal activity following peripheral inflammation.

Background

The leukotrienes (LTs) are a family of biologically active lipid mediators. They are synthesized from arachidonic acid (AA) *via* the 5-lipoxygenase pathway. AA is enzymatically converted to LTB4, LTC4, LTD4 and LTE4 that are known as bioactive LTs. LTC4, LTD4 and LTE4 are collectively termed the cysteinyl leukotrienes (CysLTs). LTs are peripherally produced by activated leukocytes in response to peripheral inflammation, such as asthma and atopic dermatitis [1,2]. Four different types (BLT1, BLT2, CysLT1 and CysLT2) of G-protein-coupled receptor for LT have been cloned [3-6]. LTB4 activates BLT1 and BLT2, and CysLTs activate CysLT1 and CysLT2.

Peripheral inflammation often elicits mechanical and thermal hyperalgesia. The most studied of these lipid mediators are the prostaglandins (PGs) of the cyclooxygenase pathway of AA metabolism [7,8]. Expression of G-protein-coupled receptors of EP for E-type PG is localized in C-fibers, unmyelinated nociceptive fibers, in the dorsal root ganglion (DRG) [8]. Activation of EP signaling plays a role in neuronal sensitization mediating modulation of the transient receptor potential vanilloid subfamily 1 (TRPV1) receptor and P2X3 receptor [9,10].

Intradermal injection of LTB4 has been shown to produce both thermal and mechanical hyperalgesia [11,12].

* Correspondence: noguchi@hyo-med.ac.jp
[1]Department of Anatomy and Neuroscience, Hyogo College of Medicine, 1-1 Mukogawa-cho, Nishinomiya, Hyogo 663-8501, Japan
Full list of author information is available at the end of the article

BioMed Central

© 2010 Okubo et al; licensee BioMed Central Ltd. This is an Open Access article distributed under the terms of the Creative Commons Attribution License (http://creativecommons.org/licenses/by/2.0), which permits unrestricted use, distribution, and reproduction in any medium, provided the original work is properly cited.

Jain et al. have reported that LTs are involved in inflammatory pain induced by carrageenan [13]. Furthermore, we demonstrated that an increase in LT synthesis in microglia in the spinal cord induced by peripheral nerve injury contributes to neuropathic pain [14]. However, in the periphery, the mechanism of the nociception induced by LTs is unknown and the precise expression pattern of LT receptors in the DRG has not been clarified. The purpose of this study is to examine the expression of LT receptor mRNAs in the DRG to assess whether LT receptors are expressed in nociceptive neurons. Furthermore, we attempted to determine the nociceptive role of LT receptors in DRG by behavioral analyses.

Results

Expression of LT receptors in the DRG

To examine whether sensory neurons express the LT receptor mRNAs, we performed reverse transcription-polymerase chain reaction (RT-PCR) and *in situ* hybridization histochemistry (ISHH) using adult rat DRG. The mRNAs for BLT1 and CysLT2 mRNAs were expressed in the DRG, but not the BLT2 and CysLT1 mRNAs (Figure 1A). For the ISHH, the BLT1 mRNA was expressed in an extremely limited population of non-neuronal cells (Figure 1B, C). With brightfield imaging of ISHH for the BLT1 mRNA, silver grains were accumulated over the non-neuronal cells whose nuclei were heavily stained with hematoxylin (Figure 1C). In contrast to the BLT1 mRNA, a subpopulation of DRG neurons expressed CysLT2 mRNA (Figure 1D, E). The darkfield photograph displayed distinguishable clusters of silver grains over the tissue with minimal background signals (Figure 1D). The brightfield and high magnification images confirmed the presence of CysLT2 on neuronal cell bodies (Figure 1E). To evaluate objectively the expression of the CysLT2 mRNA in DRG neurons, we measured, calculated, and plotted the signal-to-noise (S/N) ratio and cross-sectional area of each

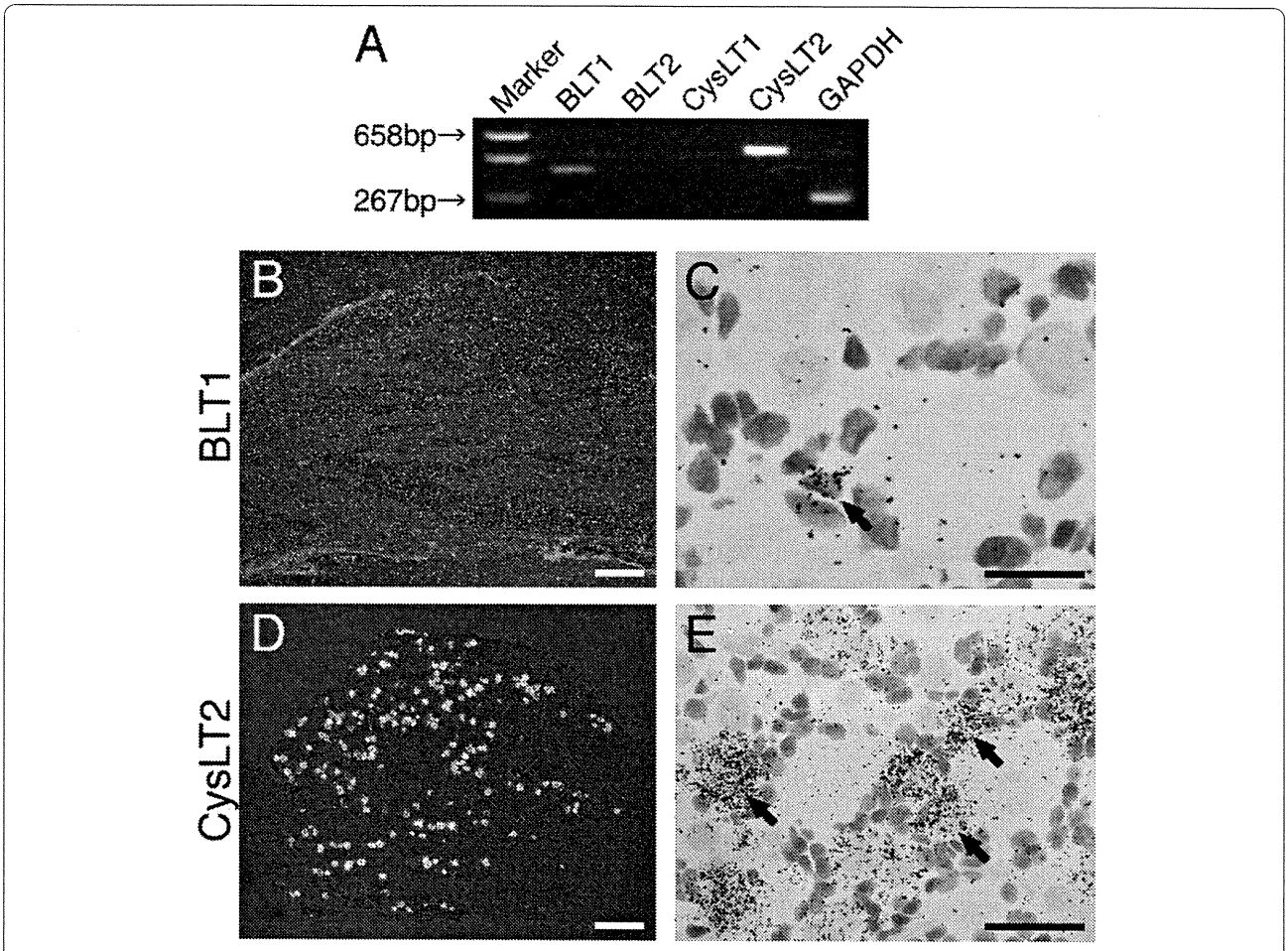

Figure 1 Expression of LT receptor mRNAs in the rat DRG. (A) The expression of mRNAs for LT receptors were determined by the RT-PCR technique. Gel panel shows PCR products from the L4, 5 DRGs taken from naive rats. (B, D) Low-magnification darkfield images of ISHH show BLT1 and CysLT2 mRNAs of naive rats, respectively. (C, E) Higher-magnification brightfield images of the left-hand images. Arrows indicate positively labeled cells by ISHH. Scale bars: B, D; 500 μm, E; 25 μm, C; 12.5 μm.

neuron (Figure 2). Based on this scattergram, neuronal profiles with a grain density of 20-fold the background level or higher (S/N ratio > 20) were considered positively labeled for this mRNA. With this criterion, 35.8 ± 3.3% of profiles were positively labeled for CysLT2 mRNA of the total DRG neurons (Table 1). The scattergram revealed that CysLT2 mRNA was expressed more intensely by the neurons with cell profiles less than 600 μm^2 compared with the medium or large-size neurons. The size distribution of the positively labeled profiles for CysLT2 mRNA is shown in Table 1. The CysLT2 mRNA was expressed in a limited population of small (< 600 μm^2) and medium-size (600-1200 μm^2) neurons, whereas large-size (> 1200 μm^2) neurons were not labeled for this mRNA (Table 1). The neuronal size definition was described previously [15].

Characterization of CysLT2-labeled neurons

To characterize the expression of CysLT2 mRNA in DRG neurons, we used double labeling ISHH with immunohistochemistry (IHC) for NF-200, a maker of myelinated A-fiber neurons. We found NF-200-immunoreactive neurons in 36.3 ± 1.5% of the total neurons (Table 2). No specific staining was observed in the absence of the primary antibody (data not shown). The results of double labeling analysis of CysLT2 mRNA with NF-200 showed that 9.6 ± 3.4% of the CysLT2 mRNA-positive profiles expressed NF-200, conversely, 8.0 ± 2.3% of NF-200-profiles expressed CysLT2 mRNA (Figure 3A; Table 2). The CysLT2 mRNA was expressed in 44.0% of NF-200 negative profiles, which were considered unmyelinated neurons (C-fiber). We tested the co-expression of CysLT2 mRNA with CGRP and IB4 in order to identify the peptide-dependent neuronal subpopulations [16], using

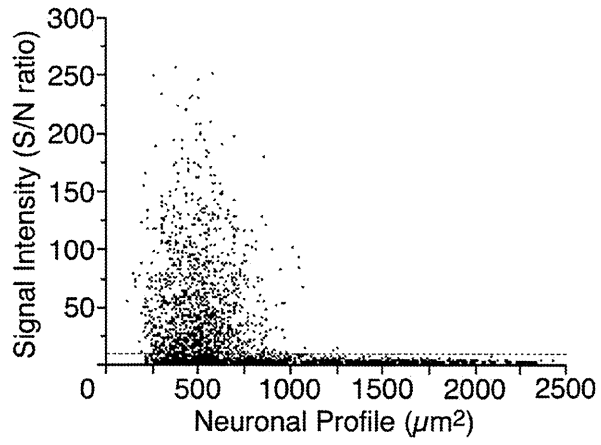

Figure 2 Scatterplot diagram of the DRG neurons expressed mRNA for CysLT2. Individual cell profiles are plotted according to the cross-sectional area and signal intensity (n = 4, 2819 cells). The dashed line indicates the borderline between the negatively and positively labeled neurons (S/N ratio = 20).

Table 1 Distribution of CysLT2 mRNA Expression in the DRG

	Small (< 600 μm^2)	Medium (600-1200 μm^2)	Large (> 1200 μm^2)
CysLT2	76.5 ± 6.5	23.5 ± 6.5	0.0 ± 0.0

Percentages of CysLT2 mRNA-expressing cells in total positive cells. Mean ± SEM (n = 4).

double labeling of ISHH with IHC. We observed CGRP-immunoreactive and IB4-binding neurons in 39.0 ± 3.1% and 37.5 ± 2.9% of the total neuronal profiles, respectively (Table 2). The results of the double labeling analysis of CysLT2 mRNA with CGRP and IB4 showed that 27.5% of the CysLT2 mRNA-positive profiles expressed CGRP; conversely, 25.6% of CGRP-profiles expressed CysLT2 mRNA (Figure 3B, Table 2), and 85.6% of the CysLT2 mRNA-positive profiles expressed IB4, conversely, 82.0% of IB4-profiles expressed CysLT2 mRNA (Figure 3C, Table 2). These results indicated that CysLT2 mRNA was expressed in non-peptidergic neurons rather than peptidergic neurons.

Next, to examine whether CysLT2 mRNA was co-expressed with TRPV1 and P2X3 that are considered as pivotal nociceptors in primary afferent fibers, we tested the percentage of colocalization of CysLT2 mRNA with TRPV1 and P2X3. We observed TRPV1 and P2X3-ir neurons in 36.7 ± 1.5% and 34.0 ± 1.9% of the total neuronal profiles, respectively (Table 2). Further, 71.2% of the CysLT2 mRNA-positive profiles expressed TRPV1; conversely, 69.6% TRPV1- positive profiles expressed CysLT2 mRNA (Figure 3D; Table 2) and 80.7% of the CysLT2 mRNA-positive profiles expressed P2X3; conversely, 88.8% P2X3- positive profiles expressed CysLT2 mRNA (Figure 3E; Table 3).

Effect of LTC4, a CysLT2 receptor agonist, on pain-related behaviors

Leukotrienes are known as proinflammatory lipid mediators, and CysLT2 was co-localized with TRPV1, a heat

Table 2 Percentages of Colocalization of CysLT2 mRNA with NF-200, CGRP, IB4, TRPV1 and P2X3 Immunoreactive Neurons in DRG

y	*x/y*	*y/x*
NF-200 (36.3%)	8.0 ± 2.3	9.6 ± 3.4
CGRP (39.0%)	25.6 ± 3.0	27.5 ± 3.9
IB4 (37.5%)	82.0 ± 4.6	85.6 ± 1.5
TRPV1 (36.7%)	69.6 ± 4.6	71.2 ± 1.8
P2X3 (34.0%)	88.8 ± 2.2	80.7 ± 3.7

x/y means the percentage of CysLT2 (x) mRNA-expressing cells in y immunoreactive cells. (number); means percentage of the neurons expressing the corresponding immunoreactivity in total DRG neurons. Mean ± SEM (n = 4).

sensor, in DRG neurons. We examined whether LTC4, a CysLT2 receptor agonist, leads to thermal hyperalgesia (Figure 4A). We tested heat sensitivity of the hind paw after intraplantar injection of LTC4 (8 fmol, 0.8 pmol and 80 pmol). None of doses affected on heat sensitivity at 10, 30 and 60 min after LTC4 injection (Figure 4A). LTC4 alone (0.8 pmol) did not contribute to the nocifensive behaviors (pain-like behaviors) and swelling of the hind paw (data not shown).

Next, because CysLT2-positive cells heavily co-localized with P2X3, we examined whether intraplantar injection of LTC4 can enhance the nocifensive behaviors induced by alpha, beta-methylene adenosine 5'-triphosphate (αβ-me-ATP), a P2X3 receptor agonist. In normal rats, αβ-me-ATP (100 μmol) consistently induced periods of intermittent hind paw-lifting behavior, which mostly began within 30-40 s after the injection and continued for the first 4 min [17]. Intraplantar injection of LTC4 at 0.8 pmol before the αβ-me-ATP injection induced a remarkable increase of paw-lifting behaviors (Figure 4B). The increase of duration of paw lifting was significantly larger than that after the injection of PBS plus αβ-me-ATP (Figure 4B). Lower and higher doses of LTC4 (< 80 fmol and 8 pmol <) did not show the alteration of nocifensive behaviors by αβ-me-ATP injection (Figure 4B). Potentiation of nocifensive behaviors induced by LTC4 showed a bell-shaped concentration-effect curve, with no significant effect at lower and higher amounts.

Table 3 Sequence Location of Primers Used in This Study

		Primer	
Gene	**GenBank Accession no.**	**Forward**	**Reverse**
BLT1	AB025230	1812-1831	2231-2212
BLT2	AB052660	488-507	939-920
CysLT1	AB052685	234-253	698-679
CysLT2	AB052661	105-124	670-651
GAPDH	M17701	80-99	350-331

Pretreatment with the LTC4 increased αβ-me-ATP-induced Fos expression

A single injection of αβ-me-ATP (100 nmol) induced Fos expression in a small number of spinal neurons (Figure 4C). The labeled neurons were in the superficial dorsal horn but were relatively distributed throughout the spinal cord laminae. The injection of αβ-me-ATP (100 nmol) into the hind paw of the LTC4 (0.8 pmol)-pretreated rats induced elevated Fos expression in spinal neurons (Figure 4D). The Fos-labeled cells were prominently observed in the medial half of the superficial laminae of the spinal dorsal horn. The number of Fos-labeled cells in laminae I-II induced by the injection of αβ-me-ATP (100 nmol) in rats pretreated LTC4 (0.8

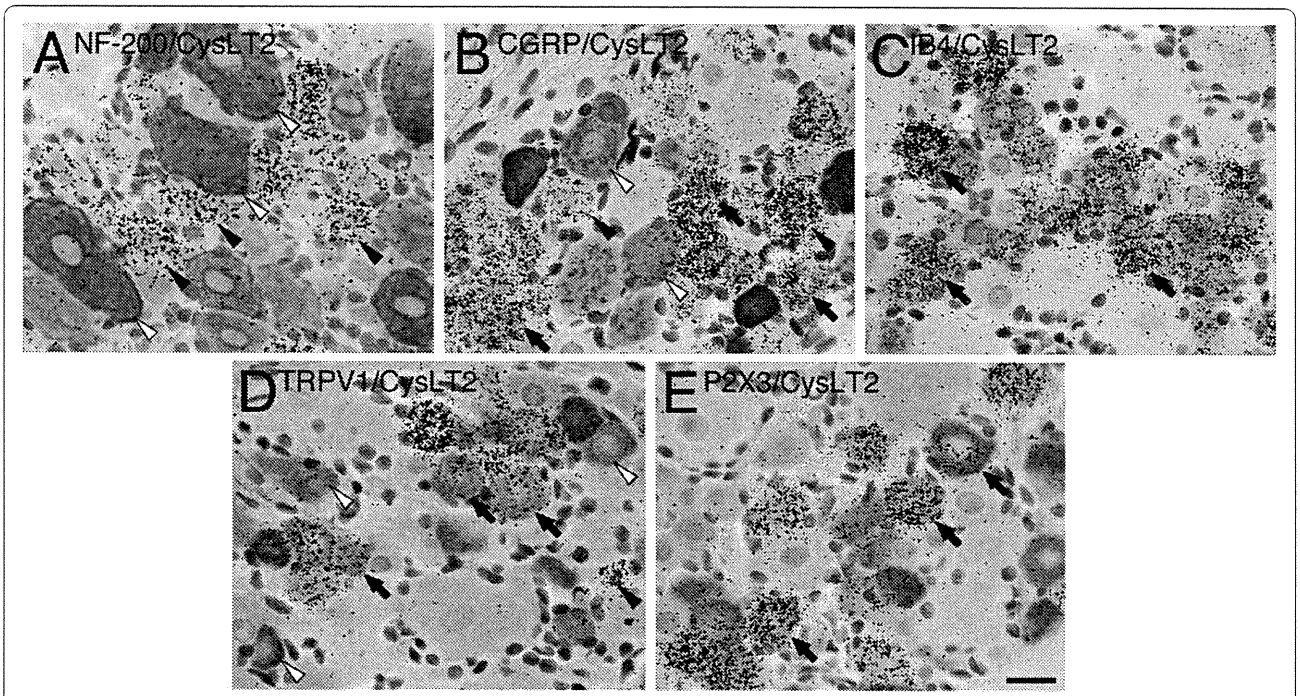

Figure 3 Distribution of CysLT2 mRNA in histochemically identified neuronal subpopulations in the rat DRG. Brightfield images of combined immunohistochemistry for (A) NF-200, (B) CGRP, (C) IB4, (D) TRPV1, (E) P2X3 with ISHH for CysLT2 mRNA. Arrows indicate examples of double-labeled cells. Solid arrowheads indicate positively labeled cells by ISHH and open arrowheads indicate examples of immunoreactive cells. Scale bars; 25 μm.

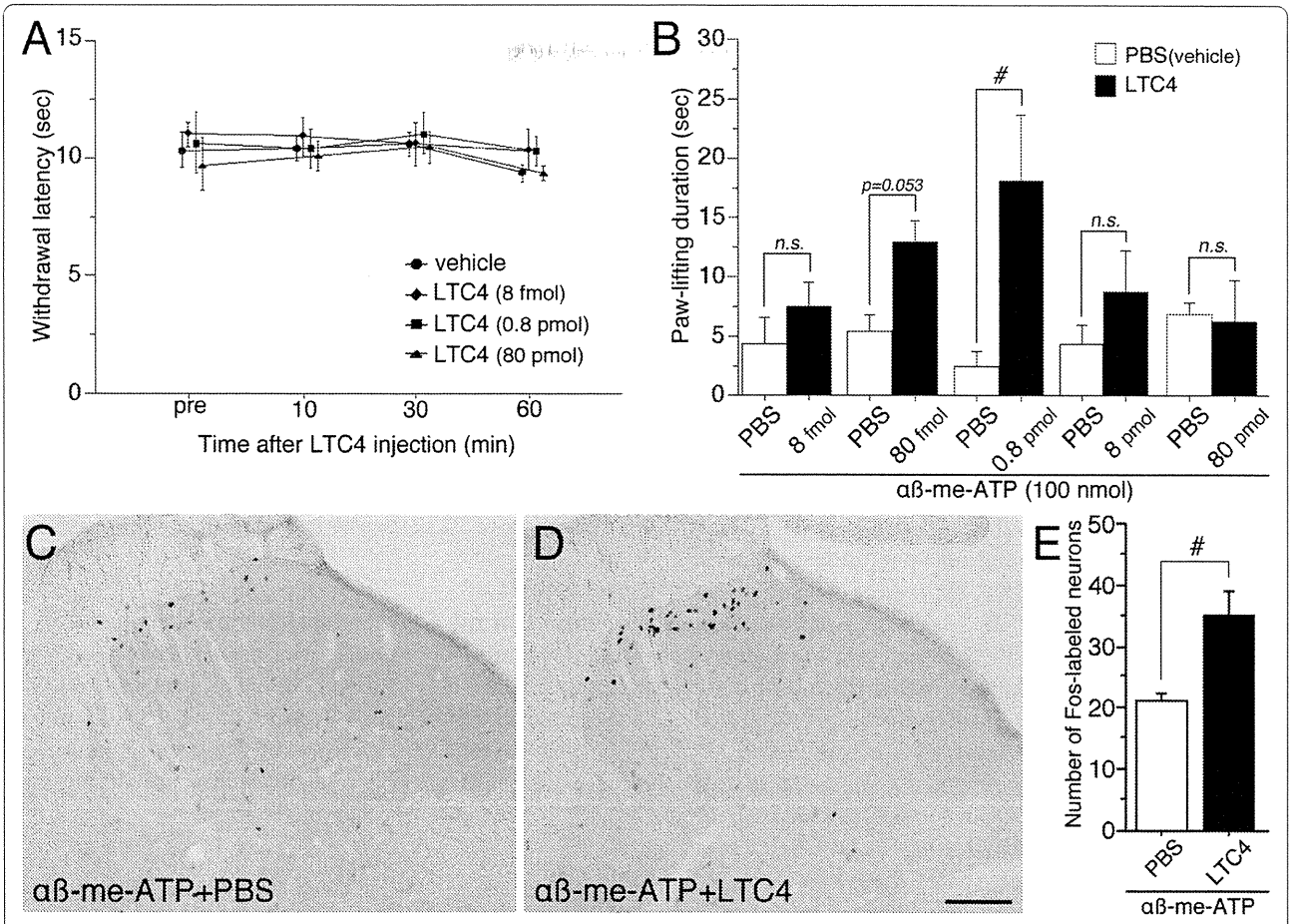

Figure 4 Effect of LTC4, a CysLT2 receptor agonist, on αβ-me-ATP induced pain behaviors and Fos expression. (A) Thermal sensitivity was evaluated by measuring withdrawal latency (sec) at pre (pretreatment), 10, 30 and 60 min after intraplantar injection of LTC4 using a plantar test. (B) The nocifensive behaviors induced by αβ-me-ATP (100 nmol) were evaluated by measuring paw-lifting duration (sec). LTC4 was given at several doses of 8 fmol - 80 pmol/paw, and the ensuing hind paw-lifting duration over the following 4 min was measured. #p < 0.05 compared with vehicle treated group. n = 4-6 for each group. (C, D) Fos protein immunoreactivity in the L5 spinal cord induced by αβ-me-ATP (100 nmol) alone (C) and LTC4 (0.8 pmol) followed by αβ-me-ATP intraplantar injection (D). (E) Number of Fos-labeled neurons in spinal laminae I-II shown in C and D. #p < 0.05 compared with vehicle treated group. n = 3 for each group. Scale bar: 100 μm.

pmol) was significantly larger (almost 1.5 times) than those pretreated with PBS (Figure 4E).

Discussion

LTs are lipid mediators with a proinflammatory profile and have been implicated in the pathogenesis of several types of inflammation [1]. For example, the blood and synovial fluids of patients with rheumatoid arthritis contain higher levels of LTB4 than people without rheumatoid arthritis [18]. LTB4 is known as a potent neutrophil chemotactic agent. It is considered that the neutrophils that are infiltrated by rheumatoid arthritis produce LTB4 in synovial fluids and induce the inflammatory condition. Several studies have demonstrated that LTs are involved in inflammatory pain [11-13]. It is well known that nerve growth factor (NGF) is up-regulated in inflammatory tissue and sensitizes nociceptors [19] leading to thermal hyperalgesia [20]. It has reported that NGF increased LTB4 in the rat paw skin and these results suggested the participation of LTB4 in NGF-induced local thermal hyperalgesia [21]. Furthermore, Trang et al. have reported that intrathecal administration of LTB4 leads to thermal hyperalgesia, and a BLT1 receptor antagonist suppresses this hyperalgesia [22]. These previous reports indicate that LTs in peripheral tissues may have an effect on primary afferents.

In the present study, we demonstrated the expression of LT receptors, BLT1, BLT2, CysLT1, and CysLT2, in the adult rat DRG. We could not detect BLT2 and CysLT1 mRNAs in the DRG. We found the BLT1 mRNA expression in non-neuronal cells, but Andoh et al. reported expression of BLT1 in mouse DRG neurons [23]. This discrepancy may be due to the difference of the species (rat versus mouse) or the methods (ISHH

versus IHC). In contrast to the expression of BLT1 mRNA, CysLT2 mRNA was expressed in DRG neurons. CysLT2 was cloned in 2000 [5], however, there has been limited information of its tissue distribution in nervous system, such as in the astrocyte in brain [24]. CysLT2 is involved in apoptosis induced by oxygen-glucose deprivation *in vitro* [24], but its functional role remains largely unknown. We precisely quantified CysLT2 mRNA in the adult rat DRG showing that about 40% of DRG neurons expressed CysLT2 mRNA (S/N > 20) and small sized DRG neurons preferentially expressed CysLT2. Double-labeling analysis with NF-200 and CysLT2 showed that most CysLT2-labeled cells did not express NF-200. Moreover, a lot of CysLT2-positive profiles exclusively co-localized with IB4-binding, a quarter of CGRP-positive neurons expressed CysLT2 mRNA. These results indicate that CysLT2 was mainly expressed in unmyelinated and non-peptidergic neurons.

Interestingly, CysLT2 mRNA expressing neurons were heavily co-localized with TRPV1- or P2X3-positive neurons. TRPV1, one of the TRPV family, has been cloned and is a thermosensitive channel with a threshold of 42 degrees Celsius [25]. TRPV1 is expressed in small sized neurons [26] and is modulated by various G-protein coupled receptors, such as EP4 [8], protease-activated receptor 2 [27] and neurokinin-1 receptor [28]*via* the protein kinase C (PKC) pathway. 12-(S)-HPETE, a product of 12-lipoxygenase, potentiates the TRPV1 current in HEK cells [29]. Thompson et al. have reported that the signaling pathway for CysLT2 is involved in the activation of PKC pathway *via* Gq-proteins [30]. Because it is possible that CysLT2 can sensitize TRPV1 in primary sensory neurons, we examined whether intraplantar injection of LTC4 leads to thermal hyperalgesia. All doses of LTC4 (8 fmol, 0.8 pmol and 80 pmol) did not affect on heat sensitivity at 10, 30 and 60 min after the injection in normal rats. The data indicate LTC4 does not have a role on thermal hyperalgesia in a normal condition. However, a further study is required to know the role of LTC4 on thermal sensitivity in tissue inflammation.

P2X3 is a ligand-gated ion channel for ATP, and belongs to P2X family. P2X3 is of particular interest in the context of pain pathways, because it is selectively expressed at high levels by nociceptors [31], and electrophysiological studies suggest that the P2X receptors in sensory neurons may play an important role in the generation and/or modulation of the pain signaling from the periphery to the spinal cord [32]. Furthermore, we previously reported that P2X3 in peripheral afferents plays a role in the induction of the hypersensitivity to mechanical stimulation observed during peripheral inflammation [33] and many P2X3s are co-expressed with protease-activated receptor 2 in the rat dorsal root ganglion neurons. Nocifensive behaviors induced by αβ-me-ATP injection to the hind paw were significantly augmented after the application of protease-activated receptor 2 agonists [17]. Fos expression induced by the αβ-me-ATP injection in dorsal horn neurons was also increased after the pre-application of protease-activated receptor 2 agonists [34]. These previous studies led us to behavioral experiments to study whether the LTC4 have a role in potentiation of pain sensation induced by αβ-me-ATP. Intraplantar injection of LTC4 before the αβ-me-ATP injection induced a significant increase of paw-lifting behaviors and Fos expression in the spinal dorsal horn. Based on the finding described in the present study, we concluded that CysLT2, the receptor of LTC4, located in the primary afferent, might modulate the activation of P2X3 by the injection of αβ-me-ATP.

Conclusions

We found that the CysLT2 is preferentially expressed by small-sized, non-peptidergic and nociceptive neurons expressing TRPV1 or P2X3 in the DRG, and contribute to the potentiation of pain behaviors induced by αβ-me-ATP. Our current observations in the context of previous findings may indicate a novel functional role of CysLT2 in the peripheral nervous system.

Methods

Experimental animals

Male Sprague-Dawley rats weighing 200-250 g were used as subjects. All animal experimental procedures were approved by the Hyogo College of Medicine Committee on Animal Research and were performed in accordance with the National Institutes of Health guidelines on animal care. Rats were used for the behavioral analyses. A few minutes after unilateral intraplantar injection of leukotriene C4 (LTC4, Cayman chemical, Ann Arbor, MI) [5S-hydroxy-6R-(S-glutathionyl)-7E,9E,11Z,14Z-eicosatetraenoic acid] [0.8 pmol-8 nmol in 50 μl of phosphate-buffered saline (PBS)], an agonist of CysLT2 receptor, the rats received intradermal injection of αβ-me-ATP (100 nmol, Sigma, St Louis, Missouri, USA) in 50 μl PBS to the plantar surface of the left hind paw. The rats were placed in a wire mesh cage immediately after the injection, and the duration of hind paw lifting during the first 4 min were measured [17,35]. For measurement of thermal hyperalgesia, the withdrawal latency (sec) of hind paw was measured from 10 to 60 min after intraplantar injection of LTC4. Thermal hyperalgesia was assessed with a plantar test (7370, Ugo Basile, Comerio, Italy). The detailed method of thermal sensitivity measurement in rat hind paw was described previously [36].

Reverse transcription-polymerase chain reaction (RT-PCR) and *in situ* hybridization histochemistry (ISHH)

The rats were killed by decapitation under deep ether anesthesia. L4 and L5 DRGs were removed and rapidly frozen with powdered dry ice and stored at 80°C until use. Extraction of total RNA was done by the single step extraction method using ISOGEN (Nippon Gene, Tokyo, Japan) that was described in a previous paper [37]. The forward and reverse primers specific for rat BLT1, BLT2, CysLT1, CysLT2 and GAPDH were designed as shown in Table 3. Amplification cycle were 33 for each cDNA. The amplified cDNA was cloned into p-GEM T-easy (Promega, MI, USA) and sequenced. These clones were used to generate the cRNA probes for ISHH.

For ISHH, the rats were killed by decapitation under deep ether anesthesia. The bilateral L4 and L5 DRGs were dissected out, rapidly frozen in powdered dry ice, and cut on a cryostat at 5 μm thickness. The protocol for ISHH was base on a publish method [38]. Using the enzyme-digested cloned, α^{35}S UTP-labeled antisense and sense cRNA probe were synthesized. Theα^{35}S-labeled probes in hybridization buffer were placed on the section, and then incubated at 55°C overnight. Sections were then washed and treated with 1 μg/ml RNase A. Subsequently, sections were dehydrated and air-dried. After the hybridization reaction, the slides were coated with NTB emulsion (Kodak, Rochester, NY, USA) and exposed for 3-4 weeks. Once developed in D-19 (Kodak), the sections were stained with hematoxylin-eosin and coverslipped.

Double labeling analysis of ISHH with immunohistochemistry (IHC)

For double labeling of ISHH with IHC, the rats were deeply anesthetized with sodium pentobarbital (70-80 mg / kg body weight, i.p.) and perfused transcardially with 100 ml of 1% paraformaldehyde in 0.1 M phosphate buffer, pH 7.4, followed by 500 ml of 4% paraformaldehyde in 0.1 M phosphate buffer. The L4 and L5 DRGs were dissected out and post-fixed in the same fixative for 4 h at 4°C, followed by immersion in 30% sucrose in 0.1 M phosphate buffer at 4°C overnight. The tissue was frozen in powdered dry ice and cut on a cryostat at 5 μm thickness. The sections were processed for IHC using the ABC method [39]. Following antibodies and binding protein were used: Mouse anti-NF200 monoclonal antiserum (1:40000, Sigma, St. Louis, MO, USA), rabbit anti-CGRP (1:10000, Amersham, Buckinghamshire, UK), isolectin B4 from *Griffonia simplicifolia* (IB4, 1:200, Sigma, St. Louis, MO, USA), rabbit anti-TRPV1 (1:100, Oncogene, Cambridge, MA, USA) and rabbit ant-P2X3 (1:500, Oncogene, Cambridge, MA, USA). The sections were washed in TBS and then incubated in biotinylated anti-rabbit or anti-mouse IgG (1:400; Vector Laboratories, Burlingame, CA, USA) in Tris buffer saline (TBS; Tris-HCl 0.1 M, NaCl 0.15 M) containing 5% serum for 2 h at 4°C, followed by incubation in avidin-biotin-peroxidase complex (Elite ABC kit; Vector, CA, USA) for 1 h at room temperature. The horseradish peroxidase reaction was developed in TBS, pH 7.4, containing 0.05% 3,39-diaminobenzidine tetrahydrochloride (Wako, Tokyo, Japan) and 0.01% hydrogen peroxidase. Sections were then washed in TBS and used for ISHH.

Immunohistochemistry for Fos expression

For Fos protein immunohistochemistry, rats were divided into two experimental groups; group 1: rats received injection of αβ-me-ATP and PBS, and were perfused 2 h after the injection; group 2: rats received injection of αβ-me-ATP and LTC4 (80 pmol) and were perfused 2 h after the injection. After appropriate survival times, the rats were deeply anesthetized and perfused transcardially with 4% paraformaldehyde described in double labeling method. L4/L5 segments of the spinal cord were removed for immunohistochemistry as described previously [40]. Rabbit primary antibody for Fos (1:20000; Ab-5; Oncogene) was used. The number of Fos-labeled neurons in laminas I-II was counted in randomly selected sections (ten out of 18-28 sections per rat). A labeled nucleus was judged as positively labeled only when a structure of appropriate size and shape indicated a clear increase in immunoreactivity above the background, but without considering intensity of the staining.

Quantitative analysis

Measurements of the density of silver grains over randomly selected tissue profiles were performed using a computerized image analysis system (NIH Image, version 1.61), where only neuronal profiles that contained nuclei were used for quantification. At a magnification of 200× and with bright-field illumination, upper and lower thresholds of gray level density were set such that only silver grains were accurately discriminated from the background in the outlined cell or tissue profile and read by the computer pixel-by-pixel. Subsequently, the area of discriminated pixels was measured and divided by the area of the outlined profile, giving a grain density for each cell or tissue profile. To reduce the risk of biased sampling of the data because of varying emulsion thickness, we used a signal-to-noise (S/N) ratio for each cell in each tissue. The S/N ratio of an individual neuron and its cross-sectioned area, which was computed from the outlined profile, was plotted. Based on this scatter gram, neurons with a grain density of ten-fold the background level or higher (20 < S/N ratio) were

considered positively labeled for CysLT2 mRNA. Because a stereological approach was not used in this study, quantification of the data may represent a biased estimate of the actual numbers of neurons. At least 500 neurons from the L4/5 DRG of each rat were measured. The number of positively labeled DRG neurons was divided by the number of neuronal profiles counted in each DRG. For IHC, only the signals that were clearly discriminative immunoreactive profiles were considered as the positive expressions.

Acknowledgements
This study was supported in part by Grants-in-Aid for Scientific Research and Grant for Pain Research Group in Hyogo College of Medicine, from the Japanese Ministry of Education, Science and Culture. We gratefully thank Dr. D.A. Thomas the correcting the English usage on this manuscript.

Author details
[1]Department of Anatomy and Neuroscience, Hyogo College of Medicine, 1-1 Mukogawa-cho, Nishinomiya, Hyogo 663-8501, Japan. [2]Department of Pharmacy, School of Pharmacy, Hyogo University of Health Sciences. Kobe, Hyogo 650-8530, Japan.

Authors' contributions
MO with KK and HY designed and performed all of experiments, analyzed data and drafted the paper. HY, KK, TF, YD and KN supervised the project and edited the manuscript. All authors contributed to data interpretation, have read and approved the final manuscript.

Competing interests
The authors declare that they have no competing interests.

Received: 21 June 2010 Accepted: 17 September 2010
Published: 17 September 2010

References

1. Sala A, Folco G: **Neutrophils, endothelial cells, and cysteinyl leukotrienes: a new approach to neutrophil-dependent inflammation?** *Biochem Biophys Res Commun* 2001, **283**:1003-1006.
2. Henderson WR Jr: **The role of leukotrienes in inflammation.** *Ann Intern Med* 1994, **121**:684-697.
3. Yokomizo T, Izumi T, Chang K, Takuwa Y, Shimizu T: **A G-protein-coupled receptor for leukotriene B4 that mediates chemotaxis.** *Nature* 1997, **387**:620-624.
4. Yokomizo T, Kato K, Terawaki K, Izumi T, Shimizu T: **A second leukotriene B (4) receptor, BLT2. A new therapeutic target in inflammation and immunological disorders.** *J Exp Med* 2000, **192**:421-432.
5. Heise CE, O'Dowd BF, Figueroa DJ, Sawyer N, Nguyen T, Im DS, Stocco R, Bellefeuille JN, Abramovitz M, Cheng R, *et al*: **Characterization of the human cysteinyl leukotriene 2 receptor.** *J Biol Chem* 2000, **275**:30531-30536.
6. Lynch KR, O'Neill GP, Liu Q, Im DS, Sawyer N, Metters KM, Coulombe N, Abramovitz M, Figueroa DJ, Zeng Z, *et al*: **Characterization of the human cysteinyl leukotriene CysLT1 receptor.** *Nature* 1999, **399**:789-793.
7. Juan H: **Prostaglandins as modulators of pain.** *Gen Pharmacol* 1978, **9**:403-409.
8. Lin CR, Amaya F, Barrett L, Wang H, Takada J, Samad TA, Woolf CJ: **Prostaglandin E2 receptor EP4 contributes to inflammatory pain hypersensitivity.** *J Pharmacol Exp Ther* 2006, **319**:1096-1103.
9. Moriyama T, Higashi T, Togashi K, Iida T, Segi E, Sugimoto Y, Tominaga T, Narumiya S, Tominaga M: **Sensitization of TRPV1 by EP1 and IP reveals peripheral nociceptive mechanism of prostaglandins.** *Mol Pain* 2005, **1**:3.
10. Wang C, Li GW, Huang LY: **Prostaglandin E2 potentiation of P2X3 receptor mediated currents in dorsal root ganglion neurons.** *Mol Pain* 2007, **3**:22.
11. Bisgaard H, Kristensen JK: **Leukotriene B4 produces hyperalgesia in humans.** *Prostaglandins* 1985, **30**:791-797.
12. Martin HA, Basbaum AI, Goetzl EJ, Levine JD: **Leukotriene B4 decreases the mechanical and thermal thresholds of C-fiber nociceptors in the hairy skin of the rat.** *J Neurophysiol* 1988, **60**:438-445.
13. Jain NK, Kulkarni SK, Singh A: **Role of cysteinyl leukotrienes in nociceptive and inflammatory conditions in experimental animals.** *Eur J Pharmacol* 2001, **423**:85-92.
14. Okubo M, Yamanaka H, Kobayashi K, Noguchi K: **Leukotriene synthases and the receptors induced by peripheral nerve injury in the spinal cord contribute to the generation of neuropathic pain.** *Glia* 2009, **58**:599-610.
15. Kobayashi K, Fukuoka T, Obata K, Yamanaka H, Dai Y, Tokunaga A, Noguchi K: **Distinct expression of TRPM8, TRPA1, and TRPV1 mRNAs in rat primary afferent neurons with adelta/c-fibers and colocalization with trk receptors.** *J Comp Neurol* 2005, **493**:596-606.
16. Snider WD, McMahon SB: **Tackling pain at the source: new ideas about nociceptors.** *Neuron* 1998, **20**:629-632.
17. Zhu WJ, Dai Y, Fukuoka T, Yamanaka H, Kobayashi K, Obata K, Wang S, Noguchi K: **Agonist of proteinase-activated receptor 2 increases painful behavior produced by alpha, beta-methylene adenosine 5'-triphosphate.** *Neuroreport* 2006, **17**:1257-1261.
18. Davidson EM, Rae SA, Smith MJ: **Leukotriene B4, a mediator of inflammation present in synovial fluid in rheumatoid arthritis.** *Ann Rheum Dis* 1983, **42**:677-679.
19. Nicol GD, Vasko MR: **Unraveling the story of NGF-mediated sensitization of nociceptive sensory neurons: ON or OFF the Trks?** *Mol Interv* 2007, **7**:26-41.
20. Ji RR, Samad TA, Jin SX, Schmoll R, Woolf CJ: **p38 MAPK activation by NGF in primary sensory neurons after inflammation increases TRPV1 levels and maintains heat hyperalgesia.** *Neuron* 2002, **36**:57-68.
21. Amann R, Schuligoi R, Lanz I, Peskar BA: **Effect of a 5-lipoxygenase inhibitor on nerve growth factor-induced thermal hyperalgesia in the rat.** *Eur J Pharmacol* 1996, **306**:89-91.
22. Trang T, McNaull B, Quirion R, Jhamandas K: **Involvement of spinal lipoxygenase metabolites in hyperalgesia and opioid tolerance.** *Eur J Pharmacol* 2004, **491**:21-30.
23. Andoh T, Kuraishi Y: **Expression of BLT1 leukotriene B4 receptor on the dorsal root ganglion neurons in mice.** *Brain Res Mol Brain Res* 2005, **137**:263-266.
24. Huang XJ, Zhang WP, Li CT, Shi WZ, Fang SH, Lu YB, Chen Z, Wei EQ: **Activation of CysLT receptors induces astrocyte proliferation and death after oxygen-glucose deprivation.** *Glia* 2008, **56**:27-37.
25. Caterina MJ, Schumacher MA, Tominaga M, Rosen TA, Levine JD, Julius D: **The capsaicin receptor: a heat-activated ion channel in the pain pathway.** *Nature* 1997, **389**:816-824.
26. Helliwell RJ, McLatchie LM, Clarke M, Winter J, Bevan S, McIntyre P: **Capsaicin sensitivity is associated with the expression of the vanilloid (capsaicin) receptor (VR1) mRNA in adult rat sensory ganglia.** *Neurosci Lett* 1998, **250**:177-180.
27. Dai Y, Moriyama T, Higashi T, Togashi K, Kobayashi K, Yamanaka H, Tominaga M, Noguchi K: **Proteinase-activated receptor 2-mediated potentiation of transient receptor potential vanilloid subfamily 1 activity reveals a mechanism for proteinase-induced inflammatory pain.** *J Neurosci* 2004, **24**:4293-4299.
28. Zhang H, Cang CL, Kawasaki Y, Liang LL, Zhang YQ, Ji RR, Zhao ZQ: **Neurokinin-1 receptor enhances TRPV1 activity in primary sensory neurons via PKCepsilon: a novel pathway for heat hyperalgesia.** *J Neurosci* 2007, **27**:12067-12077.
29. Hwang SW, Cho H, Kwak J, Lee SY, Kang CJ, Jung J, Cho S, Min KH, Suh YG, Kim D, Oh U: **Direct activation of capsaicin receptors by products of lipoxygenases: endogenous capsaicin-like substances.** *Proc Natl Acad Sci USA* 2000, **97**:6155-6160.
30. Thompson C, Cloutier A, Bosse Y, Poisson C, Larivee P, McDonald PP, Stankova J, Rola-Pleszczynski M: **Signaling by the cysteinyl-leukotriene receptor 2. Involvement in chemokine gene transcription.** *J Biol Chem* 2008, **283**:1974-1984.
31. Vulchanova L, Riedl MS, Shuster SJ, Stone LS, Hargreaves KM, Buell G, Surprenant A, North RA, Elde R: **P2X3 is expressed by DRG neurons that terminate in inner lamina II.** *Eur J Neurosci* 1998, **10**:3470-3478.
32. Burnstock G, Wood JN: **Purinergic receptors: their role in nociception and primary afferent neurotransmission.** *Curr Opin Neurobiol* 1996, **6**:526-532.
33. Dai Y, Fukuoka T, Wang H, Yamanaka H, Obata K, Tokunaga A, Noguchi K: **Contribution of sensitized P2X receptors in inflamed tissue to the**

mechanical hypersensitivity revealed by phosphorylated ERK in DRG neurons. *Pain* 2004, **108**:258-266.

34. Zhu WJ, Yamanaka H, Obata K, Dai Y, Kobayashi K, Kozai T, Tokunaga A, Noguchi K: **Expression of mRNA for four subtypes of the proteinase-activated receptor in rat dorsal root ganglia.** *Brain Res* 2005, **1041**:205-211.
35. Hamilton SG, McMahon SB, Lewin GR: **Selective activation of nociceptors by P2X receptor agonists in normal and inflamed rat skin.** *J Physiol* 2001, **534**:437-445.
36. Kobayashi K, Yamanaka H, Fukuoka T, Dai Y, Obata K, Noguchi K: **P2Y12 receptor upregulation in activated microglia is a gateway of p38 signaling and neuropathic pain.** *J Neurosci* 2008, **28**:2892-2902.
37. Yamanaka H, Obata K, Fukuoka T, Dai Y, Kobayashi K, Tokunaga A, Noguchi K: **Induction of plasminogen activator inhibitor-1 and -2 in dorsal root ganglion neurons after peripheral nerve injury.** *Neuroscience* 2005, **132**:183-191.
38. Chen ZL, Yoshida S, Kato K, Momota Y, Suzuki J, Tanaka T, Ito J, Nishino H, Aimoto S, Kiyama H, *et al*: **Expression and activity-dependent changes of a novel limbic-serine protease gene in the hippocampus.** *J Neurosci* 1995, **15**:5088-5097.
39. Yamanaka H, Obata K, Fukuoka T, Dai Y, Kobayashi K, Tokunaga A, Noguchi K: **Tissue plasminogen activator in primary afferents induces dorsal horn excitability and pain response after peripheral nerve injury.** *Eur J Neurosci* 2004, **19**:93-102.
40. Dai Y, Iwata K, Kondo E, Morimoto T, Noguchi K: **A selective increase in Fos expression in spinal dorsal horn neurons following graded thermal stimulation in rats with experimental mononeuropathy.** *Pain* 2001, **90**:287-296.

doi:10.1186/1744-8069-6-57
Cite this article as: Okubo *et al.*: Expression of leukotriene receptors in the rat dorsal root ganglion and the effects on pain behaviors. *Molecular Pain* 2010 **6**:57.

Submit your next manuscript to BioMed Central and take full advantage of:

- Convenient online submission
- Thorough peer review
- No space constraints or color figure charges
- Immediate publication on acceptance
- Inclusion in PubMed, CAS, Scopus and Google Scholar
- Research which is freely available for redistribution

Submit your manuscript at
www.biomedcentral.com/submit

BioMed Central

doi:10.1093/brain/awr025 Brain 2011: 134; 1127–1139 | 1127

BRAIN
A JOURNAL OF NEUROLOGY

JAK-STAT3 pathway regulates spinal astrocyte proliferation and neuropathic pain maintenance in rats

Makoto Tsuda,[1] Yuta Kohro,[1] Takayuki Yano,[1] Tomoko Tsujikawa,[1] Junko Kitano,[1] Hidetoshi Tozaki-Saitoh,[1] Satoru Koyanagi,[2] Shigehiro Ohdo,[2] Ru-Rong Ji,[3] Michael W. Salter[4] and Kazuhide Inoue[1]

1 Department of Molecular and System Pharmacology, Graduate School of Pharmaceutical Sciences, Kyushu University, 3-1-1 Maidashi, Higashi-ku, Fukuoka, Fukuoka 812-8582, Japan
2 Department of Pharmaceutics, Graduate School of Pharmaceutical Sciences, Kyushu University, 3-1-1 Maidashi, Higashi-ku, Fukuoka, Fukuoka 812-8582, Japan
3 Sensory Plasticity Laboratory, Pain Research Centre, Department of Anaesthesiology, Brigham and Women's Hospital and Harvard Medical School, 75 Francis Street, Medical Research Building, Room 604, Boston, MA 02115, USA
4 Programme in Neurosciences and Mental Health, Hospital for Sick Children, 555 University Avenue, Toronto, ON, Canada M5G 1X8

Correspondence to: Kazuhide Inoue, PhD,
Department of Molecular and System Pharmacology,
Graduate School of Pharmaceutical Sciences,
Kyushu University,
3-1-1 Maidashi,
Higashi-ku, Fukuoka,
Fukuoka 812-8582, Japan
E-mail: inoue@phar.kyushu-u.ac.jp

Neuropathic pain, a debilitating pain condition, is a common consequence of damage to the nervous system. Optimal treatment of neuropathic pain is a major clinical challenge because the underlying mechanisms remain unclear and currently available treatments are frequently ineffective. Emerging lines of evidence indicate that peripheral nerve injury converts resting spinal cord glia into reactive cells that are required for the development and maintenance of neuropathic pain. However, the mechanisms underlying reactive astrogliosis after nerve injury are largely unknown. In the present study, we investigated cell proliferation, a critical process in reactive astrogliosis, and determined the temporally restricted proliferation of dorsal horn astrocytes in rats with spinal nerve injury, a well-known model of neuropathic pain. We found that nerve injury-induced astrocyte proliferation requires the Janus kinase-signal transducers and activators of transcription 3 signalling pathway. Nerve injury induced a marked signal transducers and activators of transcription 3 nuclear translocation, a primary index of signal transducers and activators of transcription 3 activation, in dorsal horn astrocytes. Intrathecally administering inhibitors of Janus kinase-signal transducers and activators of transcription 3 signalling to rats with nerve injury reduced the number of proliferating dorsal horn astrocytes and produced a recovery from established tactile allodynia, a cardinal symptom of neuropathic pain that is characterized by pain hypersensitivity evoked by innocuous stimuli. Moreover, recovery from tactile allodynia was also produced by direct suppression of dividing astrocytes by intrathecal administration of the cell cycle inhibitor flavopiridol to nerve-injured rats. Together, these results imply that the Janus kinase-signal transducers and activators of transcription 3 signalling pathway are critical transducers of astrocyte proliferation and maintenance of tactile allodynia and may be a therapeutic target for neuropathic pain.

Received August 3, 2010. Revised November 21, 2010. Accepted December 19, 2010. Advance Access publication March 2, 2011
© The Author (2011). Published by Oxford University Press on behalf of the Guarantors of Brain. All rights reserved.
For Permissions, please email: journals.permissions@oup.com

Downloaded from http://brain.oxfordjournals.org/ at Aichi Medical University on May 9, 2012

Keywords: astrocytes; proliferation; STAT3; neuropathic pain; rats

Abbreviations: GFAP = glial fibrillary acidic protein; JAK = Janus kinase; p-HisH3 = phosphorylated-histone H3; STAT3 = signal transducers and activators of transcription 3

Introduction

Injury to the nervous system arising from bone compression in cancer, diabetes, infection, autoimmune disease or physical injury results in debilitating chronic pain states (referred to as neuropathic pain) (Baron, 2006). One troublesome hallmark symptom of neuropathic pain is tactile allodynia (pain hypersensitivity evoked by normally innocuous stimuli), which is refractory to currently available treatments, such as non-steroidal anti-inflammatory drugs and even opioids (Woolf and Mannion, 1999; Scholz and Woolf, 2002). Unravelling the molecular and cellular basis for the development and maintenance of pain hypersensitivity after nerve damage is therefore essential for the understanding of mechanisms underlying neuropathic pain and for the development of new therapeutic drugs.

Accumulating evidence from studies utilizing diverse animal models of neuropathic pain indicates that neuropathic pain is a reflection of the aberrant excitability of dorsal horn neurons evoked by peripheral sensory inputs (Woolf and Salter, 2000; Costigan *et al.*, 2009). This hyperexcitability might result from multiple cellular and molecular alterations in the dorsal horn occurring after peripheral nerve injury. It has long been considered that there are relevant changes in neurons, but many recent studies provide compelling evidence indicating that spinal microglia, immune-like glial cells in the CNS, rapidly respond to peripheral nerve injury and become activated with changing morphology, increasing their number and expressing a variety of genes (Watkins *et al.*, 2001; Tsuda *et al.*, 2003, 2005; Scholz and Woolf, 2007; Costigan *et al.*, 2009; Inoue and Tsuda, 2009; McMahon and Malcangio, 2009). Activated spinal microglia secrete various biologically active signalling molecules including proinflammatory cytokines (Inoue, 2006) and brain-derived neurotrophic factor (Trang *et al.*, 2009), which produces hyperexcitability of dorsal horn neurons (Coull *et al.*, 2005; McMahon and Malcangio, 2009).

Compared with rapid progress in our understanding of the microglial regulation of pain, relatively little is known about the role of astrocytes, an abundant cell type in the CNS. However, recent studies have identified signalling molecules in astrocytes that are upregulated by peripheral nerve injury such as extracellular signal-regulated protein kinase (Zhuang *et al.*, 2005), c-jun N-terminal kinase (Zhuang *et al.*, 2006), transforming growth factor-activated kinase 1 (Katsura *et al.*, 2008), S100β (Tanga *et al.*, 2006) and matrix metalloproteinase 2 (Kawasaki *et al.*, 2008). Importantly, intrathecal administration of inhibitors for these molecules reduces both peripheral nerve injury-induced hyperexcitability of dorsal horn neurons and pain behaviours (Zhuang *et al.*, 2005, 2006; Katsura *et al.*, 2008; Kawasaki *et al.*, 2008). Astrocytes receive signals from activated microglia via interleukin-18 and disrupting this interaction alleviates peripheral nerve injury-induced allodynia (Miyoshi *et al.*, 2008). These molecules are all expressed in reactive astrocytes responding to peripheral nerve injury. In addition, dorsal root injury leads to upregulation of expression of an extracellular serine protease, tissue type plasminogen activator, in spinal reactive astrocytes and inhibiting the protease reduces root injury-induced mechanical hypersensitivity (Kozai *et al.*, 2007). Therefore, it raises the possibility that the reactive process of dorsal horn astrocytes (reactive astrogliosis) may be crucial for neuropathic pain.

Although a variety of signal transduction pathways have been shown to be involved in the activation of astrocytes *in vitro*, very few signalling modules have been linked to induction of reactive astrogliosis *in vivo* (Sofroniew, 2009; Sofroniew and Vinters, 2010). Reactive astrogliosis is known as a finely graded continuum of progressive cellular and molecular changes in relation to the severity of injury and is characterized by cellular hypertrophy, hyperplasia, increased glial fibrillary acidic protein (GFAP), proliferation and, in severe cases such as spinal cord injury, scar formation (Sofroniew, 2009; Sofroniew and Vinters, 2010). Among them, proliferation is a critical process for generating numerous reactive astrocytes, which later may result in producing proinflammatory cytokines, thereby modulating dorsal horn pain processing. In contrast to cellular hypertrophy and GFAP upregulation in dorsal horn astrocytes that have been characterized in various animal models of neuropathic pain (Garrison *et al.*, 1991; Coyle, 1998; Schwei *et al.*, 1999; Tanga *et al.*, 2004; Obata *et al.*, 2006; Vega-Avelaira *et al.*, 2007), the temporal profile and molecular mechanism of proliferation of dorsal horn astrocytes and more importantly, its role in the pathological process of neuropathic pain, remains to be determined.

In the present study, we addressed these issues using the spinal nerve injury model, a well-characterized model of neuropathic pain (Kim and Chung, 1992; Tsuda *et al.*, 2003; Tanga *et al.*, 2004; Zhuang *et al.*, 2006; Kawasaki *et al.*, 2008; Miyoshi *et al.*, 2008). Here, we demonstrate for the first time that: (i) temporally restricted proliferation of dorsal horn astrocytes is induced after peripheral nerve injury; (ii) it involves the Janus kinase (JAK)-signal transducers and activators of transcription 3 (STAT3) signalling pathway; and (iii) intrathecal administration of reagents that inhibit astrocyte proliferation in rats with peripheral nerve injury produces a recovery from tactile allodynia. These results imply that astrocyte proliferation regulated by JAK-STAT3 signalling participates in the maintenance of peripheral nerve injury-induced allodynia.

Materials and methods

Animals

Male Wistar rats (250–270 g, $n = 224$, Japan SLC, Shizuoka, Japan) were used. Animals were housed in individual cages at a temperature

Downloaded from http://brain.oxfordjournals.org/ at Aichi Medical University on May 9, 2012

of 22 ± 1°C with a 12-h light-dark cycle (light on 08:30–20:30), and fed food and water *ad libitum*. All animal experiments were conducted according to relevant national and international guidelines 'Act on Welfare and Management of Animals' (Ministry of Environment of Japan) and 'Regulation of Laboratory Animals' (Kyushu University) and under the protocols approved by the Institutional Animal Care and Use committee review panels at Kyushu University.

Neuropathic pain model

We used the spinal nerve injury model (Kim and Chung, 1992) with some modifications (Tsuda *et al.*, 2003, 2009). Briefly, under isoflurane (2%) anaesthesia, a unilateral fifth lumbar spinal nerve of rats was tightly ligated by a 5-0 silk suture and cut just distal to the ligature.

Behavioural analysis

Rats were placed individually in a wire mesh cage and habituated for 30–60 min to allow acclimatization to the new environment (Tsuda *et al.*, 2003, 2009). Calibrated von Frey filaments (0.4–15g, Stoelting, IL, USA) were applied to the plantar surface of the rat hindpaw from below the mesh floor. The 50% paw withdrawal threshold was determined using the up-down method (Chaplan *et al.*, 1994). Behavioural measurements were carried out before, 1, 2, 3, 5, 7, 10, 14, 17 or 21 days after peripheral nerve injury (Figs 6A and 7B). For experiment testing, a single administration of AG490 (an inhibitor of the STAT3 activator JAK) on the established allodynia was examined on Days 3 and 5 after peripheral nerve injury (Fig. 6D and E) and the behavioural test was performed immediately before, 1, 3 and 24 h after a single bolus injection of AG490 (Fig. 6A). Locomotor activity was measured using a photobeam activity monitoring system (Chronobiology Kit; Stanford Software Systems, Santa Cruz, CA, USA) (Shinohara *et al.*, 2008), and activity counts (number of movements) were recorded for 1 h.

Drug administration to the intrathecal space

Under isoflurane (2%) anaesthesia, a 32-gauge intrathecal catheter (ReCathCo, PA, USA) was inserted through the atlanto-occipital membrane into the lumbar enlargement and externalized through the skin (Tsuda *et al.*, 2009). Four days after catheterization, the catheter placement was verified by the observation of hind limb paralysis after intrathecal injection of lidocaine (2%, 5 µl). Animals that failed to display paralysis by lidocaine were not included in the experiments. Two to 3 days after the lidocaine test, a unilateral fifth lumbar spinal nerve of rats was injured as described above. Rats were injected with either AG490 (3 and 10 nmol/10 µl, Calbiochem, CA, USA), JAK Inhibitor I, 2-(1,1-Dimethylethyl)-9-fluoro-3,6-dihydro-7 H-benz[h]-imidaz[4,5-f]isoquinolin-7-one, 2.5 nmol/10 µl, Calbiochem) or flavopiridol (5 nmol/10 µl, Santa Cruz Biotechnology, CA, USA) through the catheter once at 09:00 (AG490 and JAK Inhibitor I) or twice (once at 09:00 and once at 19:00; flavopiridol) a day from Days 3 to 5 (for immunohistochemical experiments of proliferating cells) or to Day 7 (for behavioural experiments) (Figs 5A, 6A and 7B). To examine the role of JAK-STAT3 signalling in tactile allodynia after astrocyte proliferation has finished, rats with peripheral nerve injury were intrathecally administered AG490 (10 nmol/10 µl) once a day for 5 days from Day 10 post-peripheral nerve injury (Fig. 6A). The behavioural measurements were carried out between 13:00 and 14:00 (Figs 6A and 7B) (except experiments shown in Fig. 6D and E).

Immunohistochemistry

Rats were deeply anaesthetized by intraperitoneal injection of pentobarbital (100 mg/kg) and perfused transcardially with 100 ml of phosphate-buffered saline (composition in mM: NaCl 137, KCl 2.7, KH_2PO_4 1.5, NaH_2PO_4 8.1; pH 7.4), followed by 250 ml ice-cold 4% (w/v) paraformaldehyde/phosphate buffered saline (time-line: Figs 5A and 7B). The fifth lumbar segments of the spinal cord and dorsal root ganglion were removed, post-fixed in the same fixative for 3 h at 4°C, and placed in 30% (w/v) sucrose solution for 24 h at 4°C. Transverse spinal cord and dorsal root ganglion sections (30 µm) were incubated in blocking solution (3% v/v normal goat serum) for 2 h at room temperature and then incubated for 48 h at 4°C with primary antibodies: anti-Ki-67 (rabbit polyclonal, 1:5000, Novocastra, Newcastle, UK), anti-phosphorylated-histone H3 (Ser10) (p-HisH3, rabbit polyclonal, 1:1000, Upstate/Millipore, MA, USA), anti-STAT3 (rabbit polyclonal, 1:1000, Cell Signalling, MA, USA), anti-GFAP (mouse monoclonal, 1:1000, Chemicon, CA, USA), anti-S100β (mouse monoclonal, 1:5000, Sigma-Aldrich), anti-OX-42 (mouse monoclonal, 1:1000, Serotec, Oxford, UK), anti-neuronal nuclei (mouse monoclonal, 1:200, Chemicon, CA, USA) and anti-cyclin D1 (rabbit polyclonal, 1:100, TransGenic, Kumamoto, Japan). Following incubation, tissue sections were washed and incubated for 3 h at room temperature in secondary antibody solution (Alexa Fluor™ 488 and/or 546, 1:1000, Molecular Probes, OR, USA). The tissue sections were washed, slide-mounted and subsequently coverslipped with Vectashield hardmount with 4′,6′-diamidino-2-phenylindole (DAPI; a cellular nuclear marker, 1.5 µg/ml) (Vector Laboratories, PA, USA). Three to five sections from the fifth lumbar spinal cord segments and the fifth lumbar dorsal root ganglions of each rat were randomly selected and were analysed using an LSM510 Imaging System (Zeiss, Oberkochen, Germany). Fluorescence intensities of STAT3 in ipsilateral and contralateral dorsal root ganglion sections were calculated. The numbers of $GFAP^+/S100\beta^+$ astrocytes and $Iba1^+$ microglia with clear, visible cell bodies and of p-$HisH3^+$ nuclei with a small, rounded shape (diameter ~10 µm) and a signal to noise ratio of 3.0 or more were counted. Background levels were obtained from an area in the dorsal horn of the same section where immunoreactive cells are not contained.

Real-time quantitative polymerase chain reaction

Rats were deeply anaesthetized with pentobarbital, perfused transcardially with phosphate buffered saline and the fourth to sixth lumbar spinal cord was removed immediately. Total RNA from the fourth to sixth lumbar spinal cord was extracted using Trisure (Bioline, Danwon-Gu, Korea), according to the manufacturer's protocol, and purified using the RNeasy mini plus kit (QIAGEN, CA, USA). The amount of total RNA was quantified by measuring the optical density$_{260}$ using a Nanodrop spectrophotometer (Nanodrop, Wilmington, DE). For reverse transcription, 200 ng of total RNA was transferred to the reaction with Prime Script reverse transcriptase (Takara, Kyoto, Japan) and random 6-mer primers. Quantitative polymerase chain reaction was carried out with Premix Ex Taq (Takara) using a 7500 real-time polymerase chain reaction system (Applied Biosystems, Foster City, CA) according to the manufacturer's specifications, and the data were analysed by 7500 System SDS Software 1.3.1 (Applied Biosystems) using the standard curve method. All values were normalized with to GAPDH expression. TaqMan probe, forward primer and reverse primer used in this study were designed as follows: STAT3, probe, 5′-FAM-TCGACCTAGAGACCCACTCCTTGCCAG-TAMRA-3′;

Downloaded from http://brain.oxfordjournals.org/ at Aichi Medical University on May 9, 2012

forward primer, 5′-TTGTGATGCCTCCTTGATTGTC-3′, and reverse primer, 5′-ATCGGAGGCTTAGTGAAGAAGTTC-3′; GAPDH, probe, 5′-FAM-AC CACCAACTGCTTAGCCCCCCTG-TAMRA-3′; forward primer, 5′-TGCC CCCATGTTTGTGATG-3′; reverse primer, 5′-GGCATGGACTGTGGTC ATGA-3′.

Statistics

Statistical analyses of results were evaluated using the unpaired Student's *t*-test, the Mann–Whitney U-test or the Freedman test. Analysis of the time-course of peripheral nerve injury-induced tactile allodynia between vehicle- and drug-treated groups was performed by two factors (group and times) repeated measures analysis of variance (ANOVA). Values were considered significantly different at $P < 0.05$.

Results

Proliferation activity of dorsal horn astrocytes after peripheral nerve injury

To visualize proliferating cells in the fifth lumbar dorsal horn after peripheral nerve injury induced by injury of the fifth lumbar spinal nerve, we performed immunohistochemical experiments using Ki-67, a nuclear protein expressed in all phases of the cell cycle except the resting phase (Taupin, 2007). In contrast to normal rats that only had very few Ki-67-positive (Ki-67$^+$) cells in the dorsal horn, 2 and 5 days after peripheral nerve injury a number of strong Ki-67$^+$ cells were observed in the dorsal horn ipsilateral to the injury (Fig. 1). Ki-67$^+$ cells were still observed 10 days post-peripheral nerve injury, but the number of Ki-67$^+$ cells markedly decreased (Fig. 1). To identify the type of cells positive for Ki-67, we performed double-immunolabelling for Ki-67 and for cell type-specific markers. Almost all Ki-67$^+$ cells in the dorsal horn 2 days post-injury were double-labelled with OX-42 (a microglia marker), but not with GFAP (an astrocyte marker) or neuronal nuclei (a neuronal marker) (Fig. 1B). This result is consistent with our (Inoue and Tsuda, 2009) and other previous reports (Suter *et al.*, 2007; Echeverry *et al.*, 2008) showing microglial proliferation around 2 days after peripheral nerve injury. Unexpectedly, on Day 5, we found that cells with Ki-67 immunoreactivity were not double-labelled for OX-42 or neuronal nuclei. Instead, almost all Ki-67$^+$ cells were double-labelled with GFAP (Fig. 1B), indicating proliferation of astrocytes in the dorsal horn after peripheral nerve injury.

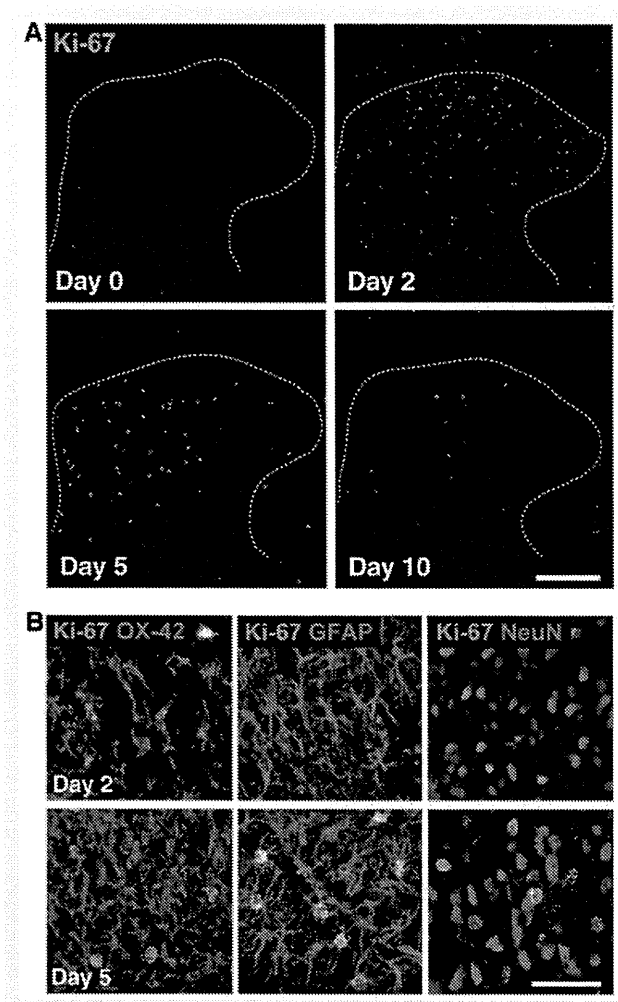

Figure 1 Immunohistochemical characterization of proliferating cells in the dorsal horn after peripheral nerve injury in rats. (**A**) Immunofluorescence of Ki-67, a nuclear protein expressed in all cell cycle phases except the resting phase, in fifth lumbar dorsal horn sections on Day 0, 2, 5 and 10 after peripheral nerve injury. (**B**) Double immunofluorescence labelling for Ki-67 (green) and cell-type markers (magenta: OX-42, microglia; GFAP, astrocytes; neuronal nuclei, neurons) in fifth lumbar dorsal horn sections on Day 2 (*upper three panels*) and Day 5 (*lower three panels*) post-peripheral nerve injury. Scale bar = 200 μm (**A**), 50 μm (**B**).

To determine the mitotic phase of cycling astrocytes, we immunostained for p-HisH3, a marker for the G_2/M phase of the cell cycle (Hendzel *et al.*, 1997; Taupin, 2007). On postoperative Day 5, strong p-HisH3$^+$ cells were seen in the dorsal horn ipsilateral to the peripheral nerve injury but not in the contralateral dorsal horn (Fig. 2A) or in the dorsal horn of control rats (data not shown). Double-immunolabelling experiments using cell markers revealed that GFAP$^+$ cells expressed p-HisH3 immunofluorescence (Fig. 2B and C). By counting p-HisH3$^+$ cells in the grey matter of the dorsal horn, we found a marked increase in the number of p-HisH3$^+$ cells on Day 5 as well as Day 2 post-nerve injury ($P < 0.05$, Fig. 2D). Consistent with our data using Ki-67, on Day 2, 86% of total p-HisH3$^+$ cells were positive for the microglial marker OX-42, and, conversely, on Day 5 a substantial proportion of p-HisH3$^+$ dividing cells were identified as astrocytes following double-labelling with GFAP (86% of total p-HisH3$^+$ cells) (Fig. 2D). The number of cells that showed p-HisH3$^+$/OX-42$^+$ and p-HisH3$^+$/GFAP$^+$ were significantly different (Day 2, $P < 0.05$; Day 5, $P < 0.01$). We further quantified the number of p-HisH3$^+$/GFAP$^+$ cells in the dorsal horn at 12-h intervals from postoperative Day 2. A marked increase in p-HisH3$^+$/GFAP$^+$ dividing cells started from 4 days after peripheral nerve injury, peaked on Day 5 and then returned to the pre-injured level over the next 5 days (10 days post-injury) (Fig. 2E). No significant

Downloaded from http://brain.oxfordjournals.org/ at Aichi Medical University on May 9, 2012

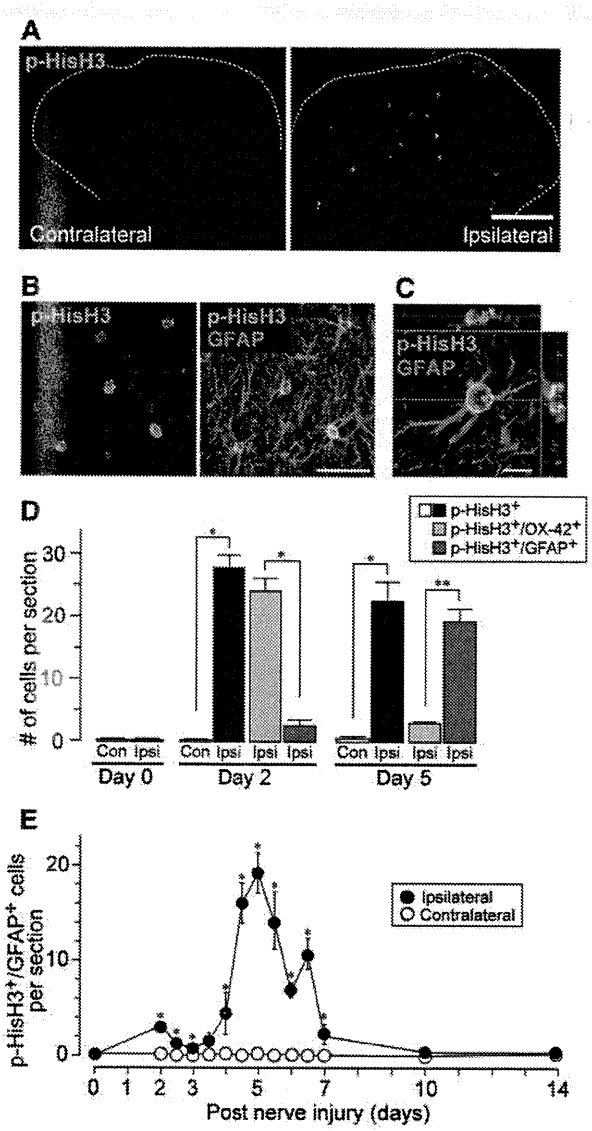

Figure 2 Mitotic phase of cycling astrocytes in the dorsal horn after peripheral nerve injury in rats. (**A**) Immunofluorescence of p-HisH3, a marker for G_2/M phase of the cell cycle, in fifth lumbar dorsal horn sections 5 days after peripheral nerve injury. (**B**) Double immunofluorescence labelling for p-HisH3 (green) and GFAP (magenta) shown in a single channel (p-HisH3, *left*) and as a merged image (p-HisH3/GFAP, *right*) from grey matter of the fifth lumbar dorsal horn 5 days after peripheral nerve injury. (**C**) Representative confocal z-stack digital images of a single cell double-immunolabelled with p-HisH3 (green) and GFAP (magenta). (**D**) The numbers of p-HisH3$^+$ cells (open and closed columns), p-HisH3$^+$/OX-42$^+$ cells (yellow columns) and p-HisH3$^+$/GFAP$^+$ cells (red columns) in fifth lumbar dorsal horn sections from rats 0, 2 and 5 days after peripheral nerve injury. Values represent the number of cells (per dorsal horn) ($n = 4$–6 rats; $^*P < 0.05$, $^{**}P < 0.01$). (**E**) The time course of p-HisH3$^+$/GFAP$^+$ cells in the dorsal horn after peripheral nerve injury. Values represent the number of p-HisH3$^+$/GFAP$^+$ cells (per dorsal horn) ($n = 3$–5 rats per each time point; $^*P < 0.05$, $^{**}P < 0.01$ versus contralateral side at the corresponding time point). Scale bar = 200 μm (**A**), 50 μm (**B**), 10 μm (**C**). Data are mean ± SEM.

change in the number of p-HisH3$^+$/GFAP$^+$ cells was observed at Days 10 and 14 (Fig. 2E). In addition, we confirmed a significant increase in the number of astrocytes (GFAP$^+$/S100β$^+$) in the ipsilateral dorsal horn on postoperative Day 7 (see below) and Days 14 and 21 (Supplementary Fig. 1). These results imply a shift of actively cycling cells from microglia to astrocytes in the dorsal horn after peripheral nerve injury, and we identified astrocytes as the principal type of dividing cell in the dorsal horn from Day 4–7 post-peripheral nerve injury.

Role of STAT3 in astrocyte proliferation in the dorsal horn after peripheral nerve injury

To explore the mechanisms regulating astrocyte proliferation, we investigated the role of STAT3 signalling. STAT3 is a principal mediator in a variety of biological processes, including cell proliferation (Levy and Lee, 2002), and there is evidence that JAK-STAT3 signalling regulates proliferation of cultured astrocytes *in vitro* (Washburn and Neary, 2006; Sarafian *et al.*, 2010). Quantitative polymerase chain reaction analysis demonstrated that the level of STAT3 messenger RNA in the spinal cord was significantly increased in the ipsilateral side on Day 5 ($P < 0.05$, Fig. 3A). By immunostaining fifth lumbar dorsal horn sections with a STAT3 antibody, we observed punctate STAT3 immunofluorescence dotted in the grey matter of the dorsal horn 5 days after peripheral nerve injury compared with the contralateral side (Fig. 3B and C). The STAT3 immunofluorescence was evident from post-nerve injury Day 3 (Fig. 3C). In contrast, STAT3 expression in the dorsal root ganglion was significantly decreased in the ipsilateral dorsal root ganglion on Day 5 post-nerve injury ($P < 0.001$, Fig. 3D and E).

To define the cells expressing punctate STAT3 immunofluorescence, we performed double-immunolabelling with cell type markers and found that almost all STAT3$^+$ cells were double-labelled with GFAP (Fig. 4A) and S100β (Fig. 4B), both of which are markers of astrocytes, but not with OX-42 and neuronal nuclei (Fig. 4C and D). STAT3 immunofluorescence accumulated in the nuclear region that was stained by DAPI (Fig. 4E). Active STAT3 is known to translocate to the nucleus (Reich and Liu, 2006), suggesting that dorsal horn astrocytes express activated STAT3 after peripheral nerve injury.

To investigate the role of STAT3 in astrocyte proliferation *in vivo*, we administered AG490, an inhibitor of the STAT3 activator JAK, intrathecally once a day for 2 days from Day 3 after peripheral nerve injury (Fig. 5A). AG490 reduced the nerve injury-induced STAT3 translocation in GFAP$^+$ astrocytes in the dorsal horn (Fig. 5B). On Day 5, the number of p-HisH3$^+$/GFAP$^+$ cells in the dorsal horn was significantly lower in AG490-treated rats than in vehicle-treated rats ($P < 0.01$, Fig. 5C and D). A similar result was obtained from rats with nerve injury treated with a JAK inhibitor (JAK Inhibitor I) ($P < 0.05$, Fig. 5D). In addition, AG490 or JAK Inhibitor I treatment resulted in a decrease in GFAP immunofluorescence in the dorsal horn 7 days after peripheral nerve injury (Fig. 5E and F).

Downloaded from http://brain.oxfordjournals.org/ at Aichi Medical University on May 9, 2012

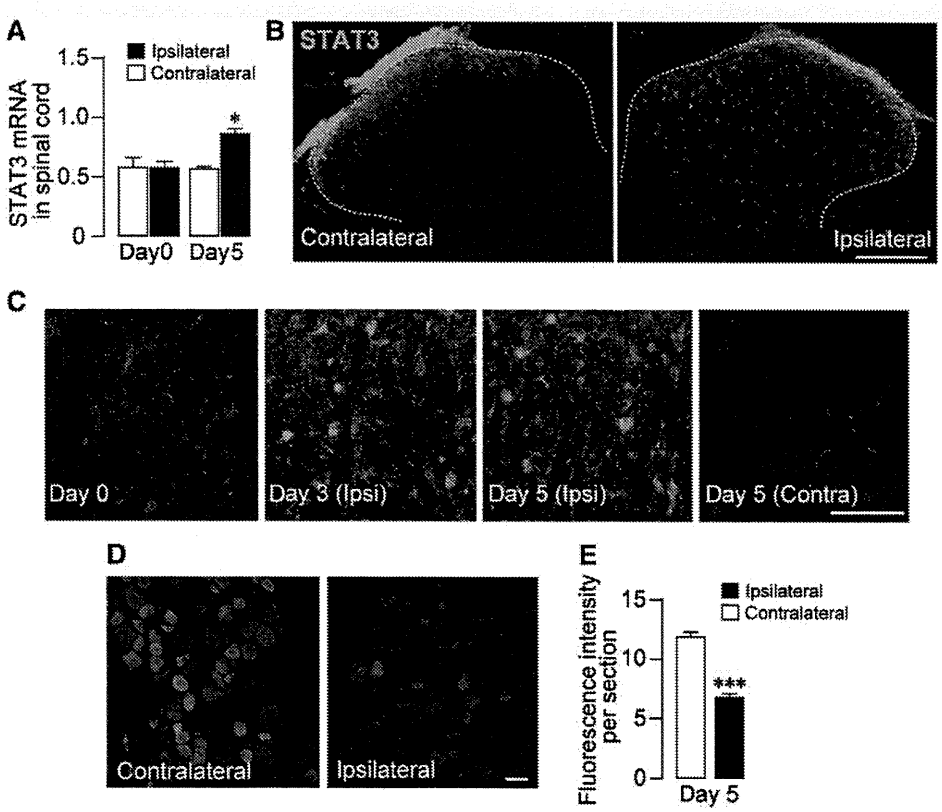

Figure 3 STAT3 expression in the dorsal horn and dorsal root ganglion after peripheral nerve injury in rats. (**A**) Real-time quantitative polymerase chain reaction analysis of STAT3 messenger RNA in the total RNA extract from the rat spinal cord ipsilateral and contralateral to the peripheral nerve injury on Day 0 and 5 after peripheral nerve injury. The levels of STAT3 messenger RNA were normalized to the value of GAPDH messenger RNA, and values represent the ratio of STAT3 messenger RNA/GAPDH messenger RNA ($n = 4$ rats; $^*P < 0.05$ versus contralateral side at the corresponding time point). (**B**) Immunofluorescence of STAT3 in fifth lumbar dorsal horn sections 5 days after peripheral nerve injury. (**C**) STAT3 immunofluorescence images at high-magnification from grey matter of the fifth lumbar dorsal horn 0, 3 and 5 days after peripheral nerve injury. (**D**) Immunofluorescence of STAT3 in fifth lumbar dorsal root ganglion sections 5 days after peripheral nerve injury. (**E**) Fluorescence intensity of STAT3 in the fifth lumbar dorsal root ganglion on Day 5 post-peripheral nerve injury ($n = 3$ rats; $^{***}P < 0.001$ versus contralateral side). Scale bar = 200 μm (**B**), 50 μm (**C**, **D**). Data are mean ± SEM.

Effect of STAT3 inhibition on nerve injury-induced tactile allodynia

To examine the role of astrocyte proliferation in nerve injury-induced tactile allodynia, we measured paw withdrawal threshold to mechanical stimulation. Rats with nerve injury (treated with vehicle) displayed a marked decrease in the paw withdrawal threshold of the ipsilateral side [$(F(6,139) = 6.165$, $P < 0.001$] but not the contralateral side (Fig. 6B). Rats with nerve injury treated with AG490 (10 nmol) from Days 3 to 7 (Fig. 6A), a regimen based on the time course of astrocyte cycling (Fig. 2E), showed a significant recovery in the decreased paw withdrawal threshold [$F(6,143) = 12.747$, $P < 0.001$; Day 5, $P < 0.05$; Day 7, $P < 0.01$; Fig. 6B]. A similar recovery from allodynia on Day 7 was observed in rats with peripheral nerve injury treated with either AG490 (3 nmol; $P < 0.01$) or JAK Inhibitor I (2.5 nmol; $P < 0.05$) (Fig. 6C). After the last administration of AG490 on Day 7, paw withdrawal threshold still remained elevated on Day 10 ($P < 0.001$, Fig. 6B). We tested the effect of acute inhibition of STAT3 signalling by a single bolus intrathecal injection of AG490 (10 nmol) on postoperative Day 3 or 5. AG490 did not produce any effect on paw withdrawal threshold over a period of 24 h (Fig. 6D and E). Notably, neither motor abnormality nor sedative effects were observed in either AG490- or JAK Inhibitor I-treated rats on Day 7 [locomotor activity (counts for 1 h): vehicle, 604.3 ± 83.8 ($n = 7$); AG490, 596.3 ± 203.5 ($n = 4$); JAK Inhibitor I, 774.3 ± 105.7 ($n = 3$)]. These results indicate that inhibiting the JAK-STAT3 signalling pathway suppresses both proliferation of dorsal horn astrocytes and the maintenance of tactile allodynia. We also examined the role of JAK-STAT3 signalling after astrocyte proliferation had finished. Intrathecal administration of AG490 for 5 days from Day 10 post-nerve injury (Fig. 6A) also significantly reduced the established tactile allodynia [$F(4,15) = 2.794$, $P < 0.05$; Days 12 and 14, $P < 0.05$, Fig. 6F]. The anti-allodynic effect of AG490 (Fig. 6F) was weaker than that of AG490 administered from Day 3 post-nerve injury (Fig. 6B),

Downloaded from http://brain.oxfordjournals.org/ at Aichi Medical University on May 9, 2012

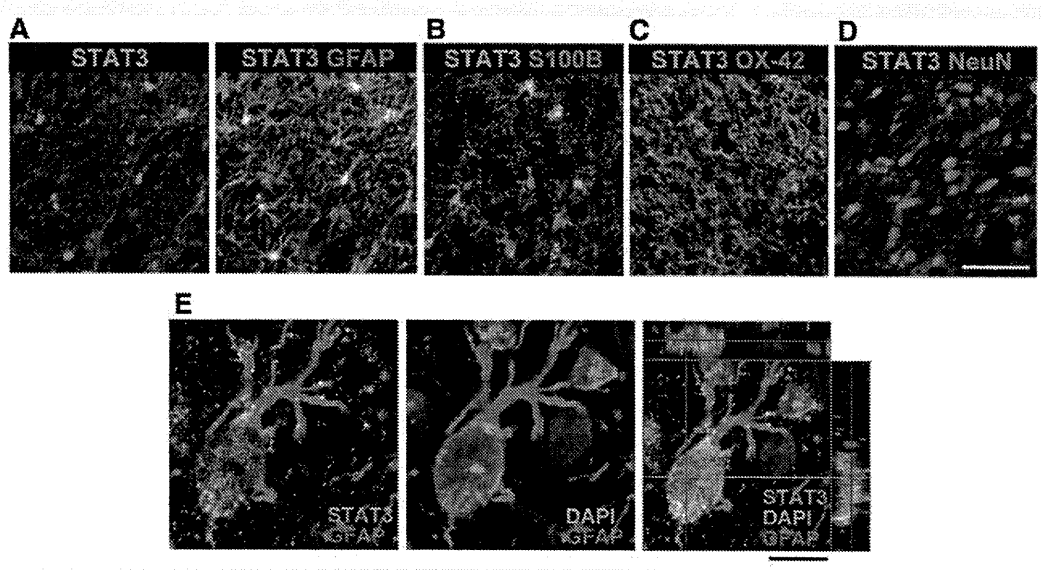

Figure 4 STAT3 translocation to the nucleus of dorsal horn astrocytes after peripheral nerve injury in rats. (**A–D**) Double immunofluorescence labelling for STAT3 (green) and cell-type markers (magenta: **A**, GFAP; **B**, S100β; **C**, OX-42; **D**, neuronal nuclei) in fifth lumbar dorsal horn sections on Day 5 post-peripheral nerve injury. (**E**) Representative confocal *z*-stack digital images of a single cell triple labelled with STAT3 (green), GFAP (magenta) and DAPI (blue) shown in double channels (*left*, STAT3/GFAP; *middle*, DAPI/GFAP) and as a merged image (*right*, STAT3/GFAP/DAPI) from grey matter of the fifth lumbar dorsal horn 5 days after peripheral nerve injury. Scale bar = 50 μm (**A–D**), 10 μm (**E**).

and after the last administration of AG490 on Day 14, the paw withdrawal threshold on Day 17 returned to the pre-injection level (Fig. 6F).

Effects of the cyclin-dependent kinase inhibitor flavopiridol on astrocyte proliferation and tactile allodynia

If astrocyte proliferation contributes to neuropathic pain, then interfering with astrocyte cycling should alleviate allodynia. To test this hypothesis, we conducted an independent test using the cell cycle inhibitor flavopiridol that inhibits astrocyte proliferation *in vitro* and *in vivo* (Di Giovanni *et al.*, 2005; Byrnes *et al.*, 2007). Flavopiridol inhibits cyclin-dependent kinases, leads to a reduction in cyclin D1 expression, and arrests cells in G_1 or at the G_2/M transition (Swanton, 2004). Because cyclin D1 is essential for astrocyte proliferation (Zhu *et al.*, 2007), we first examined cyclin D1 expression in the dorsal horn. The expression of cyclin D1 was induced in the dorsal horn 5 days post-injury (Fig. 7A), and almost all cyclin D1$^+$ cells were double-labelled with GFAP (98.6% of total cyclin D1$^+$ cells; Fig. 7A). We administered flavopiridol (5 nmol) intrathecally to rats with nerve injury twice a day for 2 days from postoperative Day 3 (Fig. 7B). The number of p-HisH3$^+$/GFAP$^+$ cells in the dorsal horn on Day 5 was significantly lower in flavopiridol-treated rats than vehicle-treated rats ($P < 0.01$, Fig. 7C and D). Furthermore, flavopiridol also significantly reduced the nerve injury-induced increase in the number of GFAP$^+$/S100β$^+$ astrocytes in the dorsal horn on Day 7 ($P < 0.01$, Fig. 7E) without affecting that of Iba1$^+$ microglia (Fig. 7F). Behaviourally, rats with nerve injury treated with flavopiridol (5 nmol) from Days 3 to 7 showed a significant recovery in the decreased paw withdrawal threshold after the injury [$F(6,44) = 3.19$, $P < 0.01$; Day 5, $P < 0.01$; Day 7, $P < 0.001$; Fig. 7G]. After the last administration of flavopiridol on Day 7, the significant attenuation of decreased paw withdrawal threshold remained on Day 10 ($P < 0.05$, Fig. 7G).

Discussion

A rapidly growing body of evidence has indicated that reactive spinal astrocytes, as well as microglia, are critical components for maintaining neuropathic pain (Watkins *et al.*, 2001; Marchand *et al.*, 2005; Tsuda *et al.*, 2005; Scholz and Woolf, 2007; Suter *et al.*, 2007; Costigan *et al.*, 2009; Hald, 2009; Inoue and Tsuda, 2009; McMahon and Malcangio, 2009; Milligan and Watkins, 2009). Despite such recent progress, very little is known about the reactive process of astrocytes in the dorsal horn after peripheral nerve injury, in particular cell proliferation, a critical process in reactive astrogliosis. In the present study, our detailed immunohistochemical analyses utilizing three independent markers of the cell cycle (Ki-67, p-HisH3 and cyclin D1) now provide compelling evidence that dorsal horn astrocytes undergo proliferation after peripheral nerve injury in rats. Consistent with previous observations using 5-bromo-2′-deoxyuridine (Narita *et al.*, 2006; Suter *et al.*, 2007; Echeverry *et al.*, 2008), these three markers also successfully detected proliferating microglia 2 days post-peripheral nerve injury, confirming the specificity of these markers. Apparently, our findings are not in line with a prevailing view that dorsal

Downloaded from http://brain.oxfordjournals.org/ at Aichi Medical University on May 9, 2012

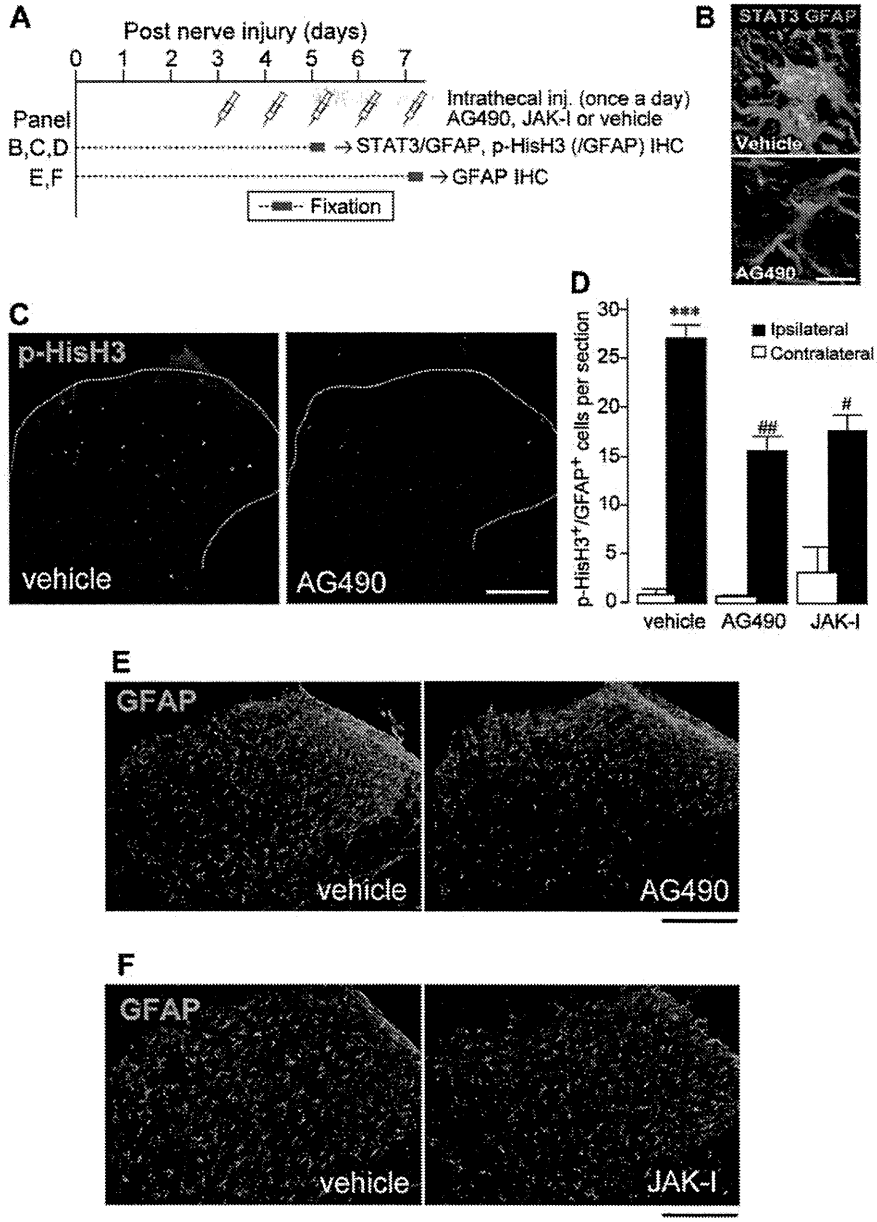

Figure 5 Role of STAT3 signalling in dorsal horn astrocyte proliferation after peripheral nerve injury. (**A**) Schematic time-line for intrathecal administration and fixation. AG490 and JAK Inhibitor I, respective inhibitors of the STAT3 activator JAK, were administered intrathecally once a day for 2 days (**B–D**) and for 5 days (**E** and **F**) from Day 3 after peripheral nerve injury. (**B**) STAT3 immunofluorescence in representative images of GFAP$^+$ cells in the fifth lumbar dorsal horn sections from vehicle- and AG490-treated rats. (**C**) p-HisH3 immunofluorescence in representative images of fifth lumbar dorsal horn sections from vehicle- and AG490-treated rats. (**D**) The numbers of p-HisH3$^+$/GFAP$^+$ cells in the fifth lumbar dorsal horn ipsilateral and contralateral to peripheral nerve injury from vehicle-, AG490- and JAK Inhibitor I-treated rats 5 days post-peripheral nerve injury. Values represent the number of p-HisH3$^+$/GFAP$^+$ cells (per dorsal horn) (n = 3–7 rats; $^{***}P < 0.001$ versus contralateral side of vehicle group; $^{\#}P < 0.05$, $^{\#\#}P < 0.01$ versus ipsilateral side of vehicle group). (**E** and **F**) GFAP immunofluorescence in representative images of fifth lumbar dorsal horn sections from rats with peripheral nerve injury treated with either vehicle, AG490 or JAK Inhibitor I on postoperative Day 7. Scale bar = 10 μm (**B**), 200 μm (**C**, **E** and **F**). Data are mean ± SEM. IHC = immunohistochemistry.

horn astrocytes do not proliferate after peripheral nerve injury (Gehrmann and Banati, 1995; Suter *et al.*, 2007; Echeverry *et al.*, 2008; Hald, 2009). However, this might be explained by the following reasons. First, these previous studies did not test proliferation activity around Day 5 post-peripheral nerve injury. Second, only the S-phase marker 5-bromo-2′-deoxyuridine, whose half-life is very short (Taupin, 2007), was used for detecting proliferating cells. Third, the present study used Ki-67 that

Downloaded from http://brain.oxfordjournals.org/ at Aichi Medical University on May 9, 2012

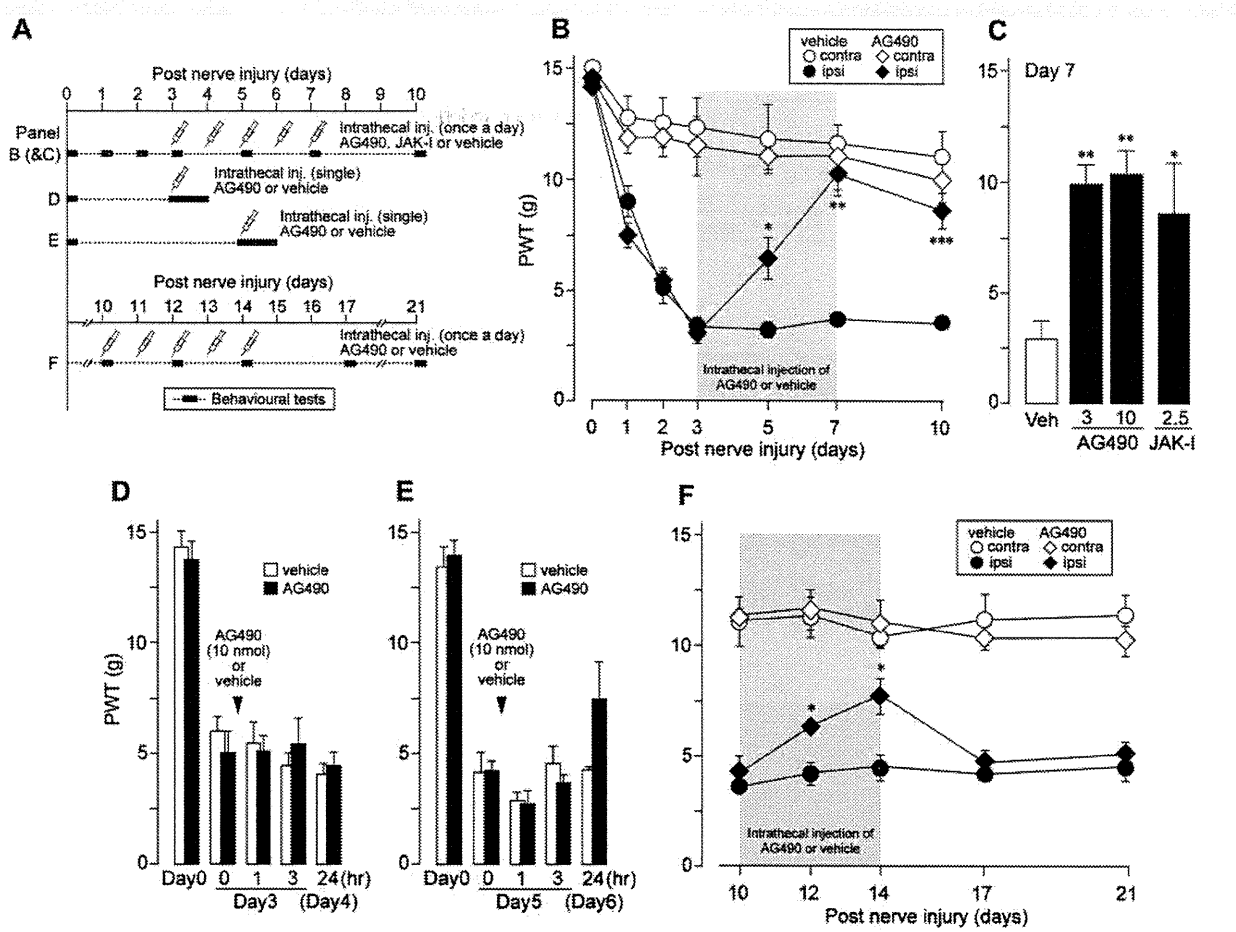

Figure 6 Recovery from tactile allodynia after peripheral nerve injury by inhibiting JAK-STAT3 signalling in rats. (**A**) Schematic time-line for intrathecal administration and behavioural tests. (**B**) Rats with peripheral nerve injury were injected intrathecally with AG490 (10 nmol/10 μl) or vehicle (10 μl) once a day for 5 days from Day 3–7. Paw withdrawal threshold (PWT) to mechanical stimulation by von Frey filaments was measured before (Day 0), 1, 2, 3, 5, 7 and 10 days after peripheral nerve injury. Values represent the threshold (g) to elicit paw withdrawal behaviour ($n = 5$ rats; $^{*}P < 0.05$, $^{**}P < 0.01$, $^{***}P < 0.001$ versus vehicle group at corresponding time point). (**C**) Paw withdrawal threshold on Day 7 in rats with peripheral nerve injury-treated intrathecally with AG490 (3 or 10 nmol/10 μl), JAK Inhibitor I (2.5 nmol/10 μl) or vehicle (10 μl) once a day for 5 days from Day 3–7. Values represent the threshold (g) to elicit PWT ($n = 5$–7 rats; $^{*}P < 0.05$, $^{**}P < 0.01$ versus vehicle group). (**D** and **E**) Paw withdrawal threshold on Day 3 (**D**) and Day 5 (**E**) in rats with peripheral nerve injury with a single bolus intrathecal injection of AG490 (10 nmol/10 μl) or vehicle (10 μl). Paw withdrawal behaviour was measured before (Day 0), pre-injection (**D**, Day 3, 0 h; **E**, Day 5, 0 h), 1, 3 and 24 h after injection. Values represent the threshold (g) to elicit paw withdrawal behaviour ($n = 4$–6 rats). (**F**) Rats with peripheral nerve injury were injected intrathecally with AG490 (10 nmol/10 μl) or vehicle (10 μl) once a day for 5 days from Days 10–14. Paw withdrawal threshold was measured 10, 12, 14, 17 and 21 days after peripheral nerve injury. Values represent the threshold (g) to elicit paw withdrawal behaviour ($n = 5$ rats; $^{*}P < 0.05$ versus vehicle group at corresponding time point). Data are mean ± SEM.

labels cells in all phases of the cell cycle except the resting phase (Taupin, 2007). Furthermore, by detecting p-HisH3^{+}/GFAP^{+} astrocytes at 12-h intervals, we could determine the temporally restricted proliferation activity of dorsal horn astrocytes after peripheral nerve injury. To our knowledge, this is the first report determining the time course of astrocyte proliferation in the dorsal horn in a model of neuropathic pain and provides evidence for changing the prevailing view.

By showing STAT3 nuclear translocation (a primary index of activation) restricted to astrocytes in the dorsal horn after peripheral nerve injury and the suppression of dividing astrocytes by JAK inhibitors, our findings further demonstrate that peripheral nerve injury-induced astrocyte proliferation in the rat dorsal horn is regulated by the JAK-STAT3 signalling pathway. Astrocytic STAT3 activation has also been observed under other neuropathological conditions accompanied by reactive astrogliosis, such as spinal cord injury (Okada *et al.*, 2006; Herrmann *et al.*, 2008), brain ischaemia (Choi *et al.*, 2003), dopamine neuron damage in the striatum (Sriram *et al.*, 2004) and facial nerve axotomy (Schwaiger *et al.*, 2000). However, there is conflicting reports that immunofluorescence of phosphorylated STAT3 increases in spinal microglia 24 h after peripheral nerve injury and, to a much lesser extent,

Downloaded from http://brain.oxfordjournals.org/ at Aichi Medical University on May 9, 2012

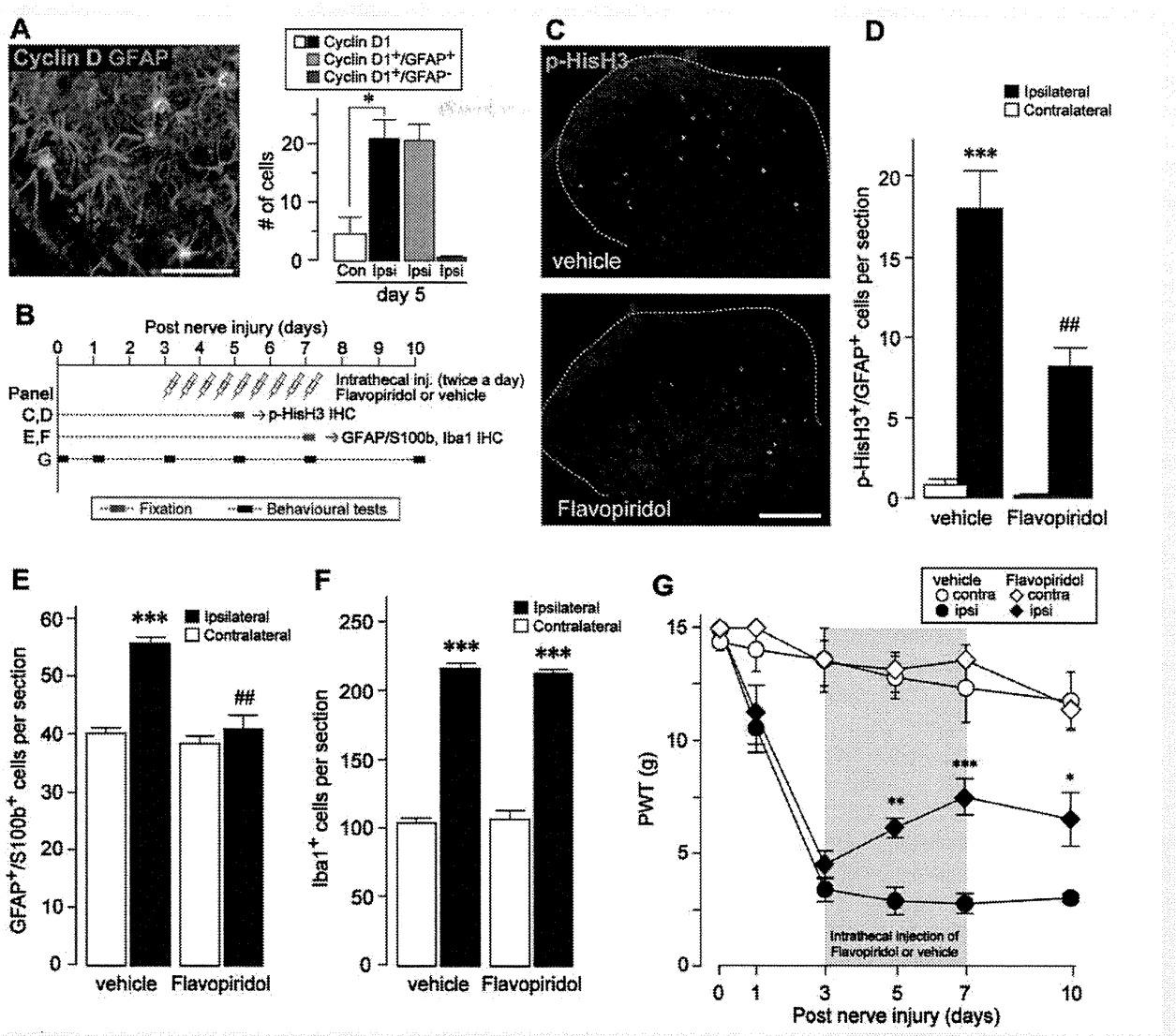

Figure 7 Effects of the cell cycle inhibitor flavopiridol on astrocyte proliferation and tactile allodynia after peripheral nerve injury. (**A**) Double immunofluorescence labelling for cyclin D1 (green) and GFAP (magenta) shown as a merged image from grey matter of the fifth lumbar dorsal horn 5 days after peripheral nerve injury. The numbers of cyclin D1$^+$cells (open and closed columns), cyclin D1$^+$/GFAP$^+$ cells (green column) and cyclin D1$^+$/GFAP$^-$ cells (dark green column) in fifth lumbar dorsal horn sections from rats 5 days after peripheral nerve injury. Values represent the number of cells (per section) ($n = 4$ rats; $^*P < 0.05$). (**B**) Schematic time-line for intrathecal administration, fixation and behavioural tests. (**C**) p-HisH3 immunofluorescence in representative images of fifth lumbar dorsal horn sections from vehicle- and flavopiridol-treated rats on Day 5 post-peripheral nerve injury. Rats with peripheral nerve injury were injected intrathecally with flavopiridol (5 nmol/10 µl) or vehicle (10 µl) twice a day for 2 days from Day 3. (**D**) The numbers of p-HisH3$^+$/GFAP$^+$ cells in the fifth lumbar dorsal horn ipsilateral and contralateral to peripheral nerve injury from vehicle- or flavopiridol-treated rats on 5 days post-peripheral nerve injury. Values represent the number of p-HisH3$^+$/GFAP$^+$ cells (per section) ($n = 5$ rats; $^{***}P < 0.001$ versus contralateral side of vehicle group; $^{\#\#}P < 0.01$ versus ipsilateral side of vehicle group). (**E** and **F**) The numbers of GFAP$^+$/S100β$^+$ (**E**) and Iba1$^+$ (**F**) cells in the fifth lumbar dorsal horn ipsilateral and contralateral to peripheral nerve injury from vehicle- or flavopiridol-treated rats on Day 7 post-peripheral nerve injury. Values represent the number of GFAP$^+$/S100β$^+$ (**E**) and Iba1$^+$ (**F**) cells (per section) ($n = 4$ rats; $^{***}P < 0.001$ versus contralateral side of vehicle group; $^{\#\#}P < 0.01$ versus ipsilateral side of vehicle group). (**G**) Paw withdrawal threshold (PWT) to mechanical stimulation by von Frey filaments was measured before (Day 0), and 1, 3, 5, 7 and 10 days after peripheral nerve injury. Rats with peripheral nerve injury were injected intrathecally with flavopiridol (5 nmol/10 µl) or vehicle (10 µl) twice a day for 5 days from Days 3 to 7. Values represent the threshold (g) to elicit paw withdrawal behaviour ($n = 5$ rats; $^*P < 0.05$, $^{**}P < 0.01$, $^{***}P < 0.001$ versus vehicle group at corresponding time point). Scale bar = 50 µm (**A**), 200 µm (**C**). Data are mean ± SEM. IHC = immunohistochemistry.

Downloaded from http://brain.oxfordjournals.org/ at Aichi Medical University on May 9, 2012